USAFA-TR-91-10

SOME RESULTS OF ADDING SOLAR RADIATION PRESSURE FORCE TO THE RESTRICTED THREE-BODY PROBLEM

STEVEN C. GORDON, LT COL, USAF

DEPT OF MATHEMATICAL SCIENCES

SEPTEMBER 1991

FINAL REPORT

APPROVED FOR PUBLIC RELEASE; DISTRIBUTION UNLIMITED

DEAN OF THE FACULTY
UNITED STATES AIR FORCE ACADEMY
COLORADO 80840

REPORT DOCUMENTATION PAGE

Form Approved
OMB No 0704 0188

1. AGENCY USE ONLY (Leave blank)	2. REPORT DATE	3. REPORT TYPE AND DATES COVERED
	7 Sep 1991	Final

4. TITLE AND SUBTITLE
Some Results of Adding Solar Radiation Pressure Force to the Restricted Three-Body Problem

5. FUNDING NUMBERS
PR 37731G

6. AUTHOR(S)
Steven C. Gordon, Lt Col, USAF

7. PERFORMING ORGANIZATION NAME(S) AND ADDRESS(ES)
Department of Mathematical Sciences
United States Air Force Academy, Colorado 80840

8. PERFORMING ORGANIZATION REPORT NUMBER
USAFATR 91-10

9. SPONSORING/MONITORING AGENCY NAME(S) AND ADDRESS(ES)
Frank J. Seiler Research Laboratory
United States Air Force Academy, Colorado 80840

10. SPONSORING/MONITORING AGENCY REPORT NUMBER

11. SUPPLEMENTARY NOTES
Research conducted under the direction of Prof K. C. Howell, School of Aeronautics and Astronautics, Purdue University

12a. DISTRIBUTION/AVAILABILITY STATEMENT

12b. DISTRIBUTION CODE

13. ABSTRACT (Maximum 200 words)

This work explores the generation of bounded orbits in the Elliptic Restricted Three-Body Problem (ER3BP), and some of the results of adding the solar radiation pressure force to the ER3BP are presented. The focus is limited to the equilibrium points defined in the Sun-Earth ER3BP. (These equilibrium points are also referred to as libration points or Lagrange points.) The addition of solar radiation pressure to the gravitational and centrifugal force structure alters the locations and conditions for linear stability of the equilibrium points in the Sun-Earth ER3BP. Solar radiation pressure also consequently affects the spacecraft orbits computed near these points. One equilibrium point in this three-body system is located between the Sun and the Earth; orbits near this point are the primary focus for the study of solar effects on the terrestrial environment and are therefore the orbits considered here.

14. SUBJECT TERMS
Libration points, three-body problem, solar radiation pressure, spacecraft orbits

15. NUMBER OF PAGES
60

17. SECURITY CLASSIFICATION OF REPORT	18. SECURITY CLASSIFICATION OF THIS PAGE	19. SECURITY CLASSIFICATION OF ABSTRACT	20. LIMITATION OF ABSTRACT
UNCLASSIFIED	UNCLASSIFIED	UNCLASSIFIED	

USAFA-TR-91-10

Technical Review by Captain Rich Schooff
Department of Mathematical Science
USAFA Academy, Colorado 80840

Technical Review by Lt Col Daryl G. Boden
Department of Astronautics
USAF Academy, Colorado 80840

Editorial Review by Lt Col Donald C. Anderson
Department of English
USAF Academy, Colorado 80840

This research report entitled "Some Results of Adding Solar Radiation Pressure Force to the Restricted Three-Body Problem" is presented as a competent treatment of the subject, worthy of publication. The United States Air Force Academy vouches for the quality of the research, without necessarily endorsing the opinions and conclusions of the author.

This report has been cleared for open publication and public release by the appropriate Office of Information in accordance with AFM 190-1, AFR 12-30, and AFR 80-3. This report may have unlimited distribution.

Robert K. Morrow Jr.

ROBERT K. MORROW JR., Lt Col, USAF
Director of Research

23 Aug 91
Dated

Accession For	
NTIS GRA&I	☑
DTIC TAB	☐
Unannounced	☐
Justification	
By	
Distribution/	
Availability Codes	
Dist	Avail and/or Special
A-1	

SOME RESULTS OF ADDING SOLAR RADIATION PRESSURE FORCE TO THE RESTRICTED THREE-BODY PROBLEM

Lieutenant Colonel Steven C. Gordon,
Assistant Professor
Department of Mathematical Sciences

PREFACE

The Elliptic Restricted Three-Body Problem (ER3BP) continues to be the focus of an increasing level of attention in the scientific community. Equilibrium points defined within a localized system of gravitational and centrifugal forces in a rotating three-body system were the subject of conside.able research during the past 200 years. More recently, spacecraft orbits near these equilibrium points have been of great interest; in particular, the ER3BP defined to include a spacecraft in orbit within the gravitational attractions of the Sun and the Earth has proven to be of great value in the study of the solar-terrestrial environment. The addition of solar radiation pressure to the gravitational and centrifugal force structure alters the locations and conditions for linear stability of the equilibrium points in the Sun-Earth ER3BP. (These equilibrium points are also sometimes referred to as libration points or Lagrange points.) Solar radiation pressure also consequently affects the spacecraft orbits computed near these points.

This work explores the generation of bounded orbits in the ER3BP, and some of the results of adding the solar radiation pressure force to the ER3BP are presented. The focus is limited to the equilibrium points defined in the Sun-Earth ER3BP, although extensions to other systems may be straightforward. One equilibrium point in this three-body system is located between the Sun and the Earth; orbits near this point are the primary focus for the study of solar effects on the terrestrial environment and are therefore the orbits considered here. This effort is supported by the Frank J. Seiler Research Laboratory and has been conducted as doctoral research under the direction of Professor K.C. Howell, School of Aeronautics and Astronautics, Purdue University, West Lafayette, Indiana.

TABLE OF CONTENTS

page

TABLE OF CONTENTS.....iii

LIST OF FIGURES.....v

CHAPTER 1: INTRODUCTION.....1

A. Definition of the Problem.....2

B. Previous Contributors.....4

1. The Many-Body Problem.....4

2. The Three-Body Problem.....6

3. Libration Point Orbits.....7

a. Historical Background.....7

b. One Objective of Sun-Earth Libration Point Orbital Missions.....10

c. Some Missions Planned in the Sun-Earth System.....11

d. Halo Orbits.....12

e. Lissajous Orbits.....15

C. Overview.....17

CHAPTER 2. RESULTS.....18

A. Elliptic Restricted Three-Body Problem.....18

B. Coordinate Systems.....19

page

C. Equations of Motion.....19

D. Locations of the Lagrangian Points.....31

1. The CR3BP.....31

2. The ER3BP.....35

E. State Transition Matrix.....41

F. Bounded Orbits Near Libration Points.....44

1. Stability of the Libration Points in the CR3BP.....45

2. Stability of the Libration Points in the ER3BP.....48

3. Construction of Bounded Collinear Libration Point Orbits.....47

4. Reference Paths Used in This Work.....54

CONCLUSION.....57

REFERENCES.....58

LIST OF FIGURES

Figure Page

1-1....Libration Point Locations in the CR3BP.....3

1-2....An Orthographic Depiction of a Halo-Type Orbit.....14

1-3....An Orthographic Depiction of a Lissajous Orbit.....16

2-1....Coordinate Systems With Barycenter Origin.....20

2-2....Lagrange Point Locations in the Scaled CR3BP.....32

2-3....Lagrange Point Locations in the Scaled ER3BP.....40

2-4....Three Orthographic Views of a Lissajous Orbit.....55

2-5....Three Orthographic Views of a Halo-Type Orbit.....56

CHAPTER 1: INTRODUCTION

With the expansion of space exploration programs worldwide, interest has increased in the design of innovative, complex, and yet low-cost spacecraft trajectories that meet demanding mission requirements. In most of the missions flown in the last few decades, the spacecraft spent the majority of the flight time in a force environment dominated by a single gravitational field. For the preliminary mission analysis in these cases, additional attracting bodies and other forces could be modeled, when required, as perturbing influences. Analysis of some recently proposed and more adventurous missions, such as those involving libration point orbits, will require dynamic models of higher complexity, since at least two gravitational fields are of nearly equal influence on the spacecraft throughout the majority of the mission. Thus, trajectories determined for a system consisting of numerous gravitational forces have been of particular theoretical and practical interest in recent years.

One type of many-body problem, motion within a three-body system of forces, has a wide range of applications. The general problem of three bodies assumes that each body has finite mass and that the motion is a result of mutual gravitational attraction. When the mass of one of the three bodies is assumed to be sufficiently small (infinitesimal) so that it does not affect the motion of the other two bodies (primaries) in the system, the "restricted three-body problem" results. The primaries can be further assumed to be moving in known elliptic or circular orbits about their common center of mass. Therefore, the elliptic restricted three-body problem, where the primaries are assumed

to be in known elliptic orbits, may be considered a reasonably approximate model for a spacecraft moving within the gravitational fields of the Sun and the Earth, for instance.

A. Definition of the Problem

In the formulation of the restricted three-body problem, one mass is defined as infinitesimal relative to the remaining two masses (primaries). The primaries, unaffected by the infinitesimal mass, move under their mutual gravitational attractions. In the elliptic restricted three-body problem (ER3BP), the primaries are assumed to move on elliptic paths. If the eccentricity of the primaries' orbit is assumed to be zero, the circular restricted three-body problem (CR3BP) results. Even for known primary motion, however, a general, closed-form solution for motion of the third body of infinitesimal mass does not exist. In the restricted three-body problem (ER3BP or CR3BP), five equilibrium (libration) solutions can be found. These equilibrium points are particular solutions of the equations of motion governing the path of the infinitesimal mass moving within the gravitational fields of the primaries.

The equilibrium points are defined relative to a coordinate system rotating with the primaries. At these locations, the forces on the spacecraft are in equilibrium. These forces include the gravitational forces from the massive bodies and the centrifugal force associated with the rotation of the system. (The addition of solar radiation pressure to the force model changes the locations of the five Lagrange points, although they can still be defined, and these solar radiation effects will be discussed in the next chapter.) The five libration points are located in the plane of primary rotation and are depicted in Figure 1-1 for the CR3BP. Three of the libration points are on the line between the two massive bodies, and one of these collinear points

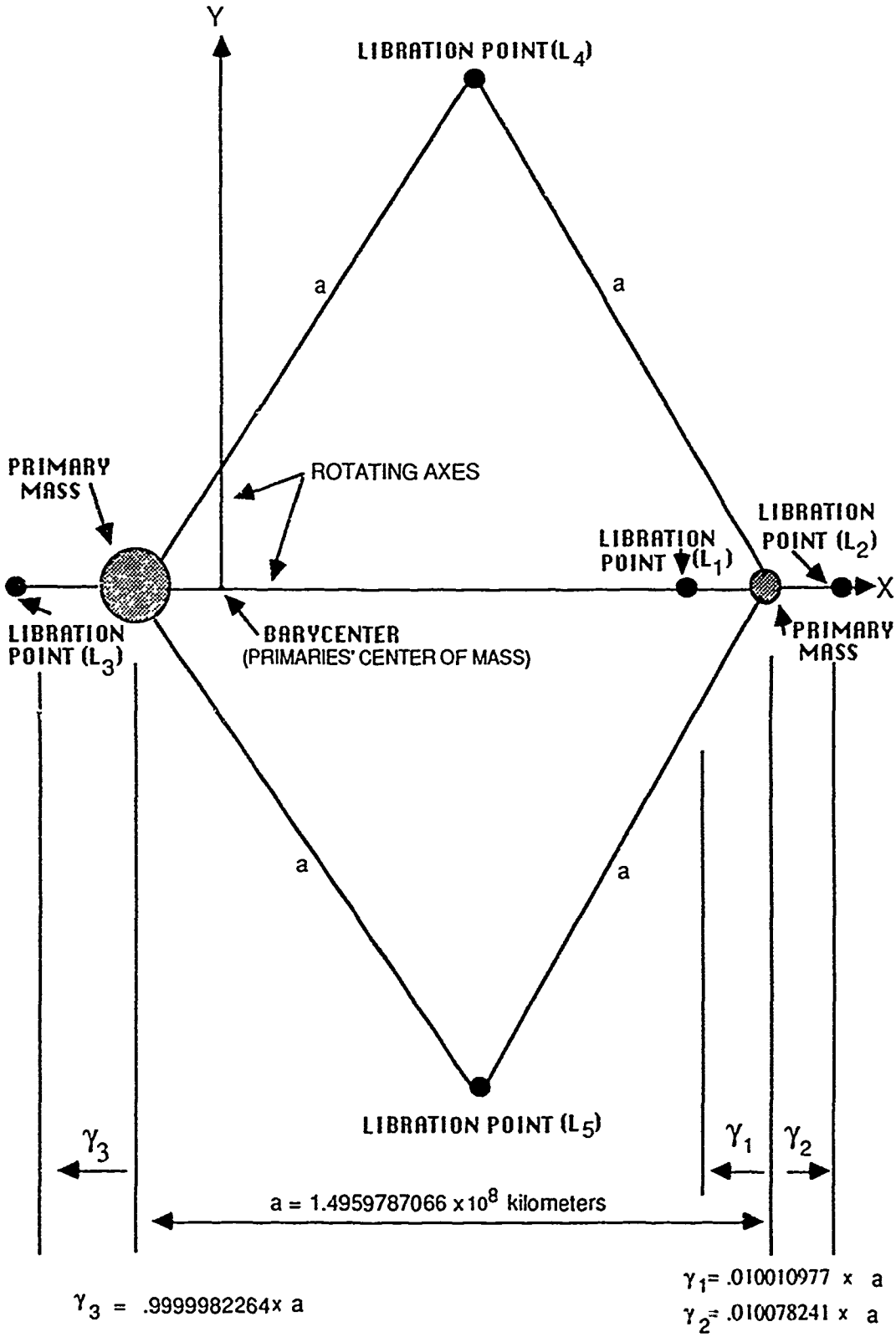

Figure 1-1. Libration Point Locations in the CR3BP.

is interior to the primaries. The last two points are at the vertices of two equilateral triangles in the plane of primary rotation. The triangles have a common base that is the line between the primary masses.

For the CR3BP, the five libration points are stationary relative to the rotating reference frame. The approximate relative distances between the primaries and the five libration points are also given in Figure 1-1. If the problem is generalized to the ER3BP, the libration points pulsate as the distance between the primaries varies with time. In both the circular and the elliptic restricted problems, two-dimensional and three-dimensional trajectories, both periodic and quasi-periodic paths, can be computed in the vicinity of these libration points.

B. Previous Contributors

The formulation and solution of the equations of motion governing two or more heavenly bodies moving under the influence of their mutual gravitational fields have inspired many researchers through the centuries. The difficulty involved in finding any solution to the multi-body problem has been fortunate for the development of the mathematics, science, and engineering methods used in the investigations. A few of the many significant contributions are mentioned briefly here. The problem history is described in terms of the many-body problem, the three-body problem, and then libration point orbits that include both periodic and quasi-periodic trajectories.

1. The Many-Body Problem

Even the simplified two-body problem successfully investigated by Johanness Kepler was not, in fact, simple to solve. Kepler's laws of planetary motion, published between 1609 and 1619, did not account for

the masses of the two planets and assumed that the planets move on elliptical paths about the Sun. The findings of Kepler were a major development in that they supported the heliocentric theory, which documented evidence suggests was first postulated by Aristarchus of Samos in Ancient Greece and then rediscovered by Nicholas Copernicus (1473-1543).

Sir Isaac Newton (1642-1727) was first to formulate the many-body problem as three or more massive particles moving under their mutual gravitational attractions. Other researchers, including Kepler, had proposed the concept of the inverse square law of gravitation, but Newton's many scientific discoveries included his recognition that the inverse square law of gravitation was the fundamental law of celestial mechanics. However, even with the planets modeled as point masses, finding any solution to the problem involving three or more bodies is nontrivial.

Leonhard Euler (1707-1783) showed that ten integrals of the motion (ten constants of integration) exist in the many-body problem. Six of these scalar constants result because total linear momentum is conserved. Three of the scalar constants of integration result from the conservation of total angular momentum. The tenth constant is due to the conservation of total mechanical energy of the system of bodies. Euler was the first to use mathematical methods, rather than the accepted geometrical approaches of his time, to solve problems in dynamics, and he is therefore widely considered to be the father of analytical dynamics. Many years later, Henri Poincaré (1854-1912) significantly concluded, along with others, that no additional integrals exist in the many-body problem if three conditions hold: (1) the integrals of the motion are equations involving only integral or algebraic functions of the coordinates and velocities of the bodies in question, (2) they are valid for all values of the masses, and (3) they satisfy the equations of motion. Poincarè had extended and generalized the work of H. Bruns whose findings were published in 1887 and described specific necessary conditions for the existence of integrals of the motion for the general problem of three bodies.

The set of differential equations governing motion in the many-body problem includes a second-order vector differential equation for each body. When n bodies are defined, 3n second-order scalar differential equations result. In order to completely specify the motion of these n particles, 6n constants of integration are required. Since Euler showed that 10 integrals exist and Poincaré proved that only the 10 (with certain restrictions on form) can exist, a three-body problem that requires 18 constants of the motion would thus defy general closed-form solution. By eliminating time as the independent variable and by using an "elimination of the nodes" method originally developed by Carl Gustav Jacobi (1804-1851), the many-body problem may be reduced to order 6(n-2). The general three-body problem would still have six unknown constants of the motion. It is intriguing that the general three-body problem looks deceptively similar to the general two-body problem, yet the general problem of three bodies is of a much higher degree of complexity and does not have a general closed-form solution.

2. The Three-Body Problem

The three-body problem has long been a rich research area in celestial mechanics. Newton studied and found some approximate solutions to the general problem of three bodies. In 1765, Euler solved the problem of three massive bodies that maintain a constant ratio of their relative distances from each other and move on a fixed straight line. Later, Joseph-Louis Lagrange presented his particular solutions of the general three-body problem in 1772. Lagrange, a student and friend of Euler, found five equilibrium (libration) points in the general three-body problem. These five libration points are thus also referred to as Lagrange points. Pierre-Simon de Laplace repeated Lagrange's analysis in his works published between 1799 and 1825. Joseph Liouville (1809-1882) studied the Sun-Earth-Moon three-body problem in particular. Liouville investigated the

instability of the three-body configuration and the effects of disturbing forces on the Moon's motion. He proved that the collinear libration (or Lagrange) points are unstable points of equilibrium. The two triangular points have been found to be linearly stable for certain ratios of the primary masses and for certain values of primary orbit eccentricity. George W. Hill also studied the motion of the Moon in the Sun-Earth-Moon system and published his theory of lunar motion in 1378.

The "restricted" problem of three bodies has been of great research interest in the last 100 years. Poincaré was apparently the first researcher to coin the term "restricted" to refer to the problem in which the infinitesimal mass is assumed to have no effect on the movement of the finite masses. The primary masses may be assumed to be in either circular or elliptic orbits, and the motion of the infintesimal mass in the vicinity of a Lagrange point can then be studied.

3. Libration Point Orbits

In this section, a brief historical background of libration point orbital research is presented. Then, one goal of the continuing scientific investigations concerning libration point orbits in the Sun-Earth system is discussed. The third part of this section describes several planned missions in the Sun-Earth system. The final two subjects discussed are periodic (halo) and quasi-periodic (Lissajous) orbits, respectively.

a. Historical Background

Libration point orbits have been the subject of considerable research interest. Poincaré completed significant work on bounded periodic orbits that were two-dimensional (orbits of his first and

second kind) in the CR3BP and the ER3BP (respectively) and that were three-dimensional (orbits of his third kind) in the CR3BP. He looked at families of periodic orbits indexed by the ratio of the mass of the smaller primary to the sum of the primary masses. Works by Sir George Howard Darwin (son of Charles Darwin) in 1899 and 1911 investigated the circular restricted three-body problem. His studies included the stipulations that the infinitesimal mass remained in the plane of motion of the primaries and that one primary was ten times as massive as the other.[1,2] Darwin numerically calculated a number of periodic orbits in the planar CR3BP. (Of course, numerical integration computations at that time were highly labor-intensive.) Karl Frithiof Sundman obtained a general solution using convergent series for the general problem of three bodies in 1912, but the slowness of convergence made it of little practical value.[3,4] Henry Crozier Plummer published works in 1903 and 1914 concerning approximate analytic solutions to the planar CR3BP.[5,6] Forrest Ray Moulton described the problem in his 1914 book and analyzed a great variety of periodic orbits and approximate analytic solutions in the planar CR3BP in 1920.[7,8]

Several additional scientific discoveries and research accomplishments in this century helped to spur interest in libration point orbits. Until the early twentieth century, investigations concerning the five Lagrangian points had been considered interesting but purely academic.[4] It had seemed highly unlikely that such unusual planetary formations could exist in nature. Then, in 1906, a small planet in the Sun-Jupiter three-body system was found to be moving in close proximity to one of the triangular libration points. This small planet is named Achilles and is one of the Trojan asteroids that now have been found to number approximately 25. Before the 1950s, solutions were also constrained to hand calculations and analytic approximations. A 1966 book by Victor Szebehely thoroughly summarized the evolution of efforts to understand the three-body problem to that date.[9] Until then, most of the work of generating solutions had been limited to two-dimensional orbits in the plane of motion of the

primaries. Within the past 30 years, high speed, electronic computing devices helped make more accurate numerical solutions possible and enabled the study of three-dimensional trajectories.

More recently, the discovery of other objects orbiting in the vicinity of libration points has also helped to increase interest. Analysis of data from the Voyager 1 spacecraft found that two of Saturn's moons complete the Saturn-Dione A-Dione B equilateral triangle solution for that three-body system. The two moons are the same distance from Saturn, and the much smaller Dione B slowly oscillates near a point that remains some 60° ahead of Dione A as the moons orbit around Saturn. Some meteoric dust particles are also suspected to be orbiting near the triangular libration points in the Earth-Moon system.[4,9] In the Sun-Earth system, the collinear libration point on the dark side of the Earth may be the location of meteoric dust particles that can be seen to reflect light from the setting Sun.[4,7,9] The discoveries of, and speculations about, these natural formations located in the vicinity of Lagrange points, and the increasing capabilties of electronic computers, have facilitated interest in orbits for artificial satellites near these points.

The circular or elliptic motion of the primaries, as modeled in the CR3BP or ER3BP, may be considered a good orbital approximation. The orbit of a planet about the Sun or the orbit of the Moon about the Earth is approximately Keplerian, and the spacecraft can easily be considered an infinitesimal mass in comparison. The study of libration point orbits in such systems is gaining in significance because the positioning of spacecraft near Earth-Moon or Sun-Earth libration points can be of value to meet a number of objectives. Earth-Moon equilateral libration points have been studied for potential stationing of space colonies and transportation relay stations. The translunar libration point in the Earth-Moon system has also been proposed as the location of a communications relay satellite to support a lunar exploration base on the far side of the Moon. The Sun-Earth interior libration point is a site of great interest for upstream investigation of solar effects on the Earth. One mission, the International Sun-Earth Explorer-3,

successfully conducted such scientific research while in a libration point orbit for nearly 4 years. Scientific interest, then, continues to motivate Sun-Earth libration point trajectory studies; in part, because solar activity has some remarkable--and damaging--influence on the Earth's atmosphere.

b. One Objective of Sun-Earth Libration Point Orbital Missions

One important goal of some Sun-Earth libration point orbital research is to study solar effects on the terrestrial environment. The ceaseless solar wind contains a constant stream of particles stripped from the Sun; however, it is the unexpected solar storms that do the greatest amount of harm on Earth. The unpredictable solar eruptions release sudden surges of particles into the solar wind, and the particles reach the Earth some 4 days later (they travel at approximately 1.5 million kilometers per hour).[10] The surge in particles can cause a geomagnetic storm that upsets delicate electronics and that can damage electrical supply systems. Changes in the Earth's magnetic field (caused by the geomagnetic storm) can induce quasi-direct currents in high-voltage alternating current transmission lines and can thus damage transformers.[10] In March 1989, a surge of particles hit the areas near the North Pole and caused a blackout in Canada's province of Quebec and the shutdown of a nuclear power plant in New Jersey. Two hundred electrical utilities were in some measure affected by this solar storm.[10]

Significantly, there are additional major terrestrial changes as a result of the unpredictable solar storms. Increased solar radiation also causes the Earth's outer atmosphere to expand. The outer atmospheric expansion, in turn, increases the drag on some satellites, thus degrading their attitude control and changing their orbital tracks. In 1989, the United States Air Force Space Command temporarily lost track of approximately 1,400 space objects for up to several weeks as increased drag due to solar-induced terrestrial atmospheric

expansion changed their previously-predicted paths.[10] The solar-induced atmospheric expansion near the Earth has also caused the Soviet Salyut 7 space station to plunge to Earth in 1991, some 3 years early. The Soviets had boosted it to a higher orbit from where it should have continued orbiting until approximately the year 1994; however, the increased atmospheric drag changed its orbital path and caused it to begin an uncontrolled tumble.

Unfortunately, these solar storms are not well predicted. Ground-based solar storm warning systems are inadequate; in fact, currently only 14% of the storms are preceeded by an accurate warning, and the existing warning system provides a 78% false alarm rate.[10] One of the several objectives of future libration point orbit research in the Sun-Earth system could then be the study of solar storms and the potential use of storm warning spacecraft. Positioning of a warning spacecraft near the Sun-Earth interior Lagrange point will allow about an hour's notice of an incoming solar storm.

c. Some Missions Planned in the Sun-Earth System

Future spacecraft missions will increase scientific knowledge of the solar-terrestrial environment and are planned as collaborative efforts of several agencies. The National Aeronautics and Space Administration (NASA), the European Space Agency (ESA), and the Institute of Space and Astronautical Science (ISAS) in Japan are the major participants, with some minor involvement of the United States' Department of Defence (DoD), in this solar-geospace research.[11]

Several planned missions are part of the joint International Solar-Terrestrial Physics (ISTP) program. A mission designated as WIND is scheduled for launch on December 22, 1992; following a 2-year double-lunar swingby trajectory, WIND will be injected into a libration point orbit between the Earth and the Sun in January 1995.[12] The Solar and Heliospheric Observatory (SOHO) Mission is currently scheduled for launch on March 14, 1995.[12] SOHO will be placed into

orbit near the libration point between the Earth and the Sun, and its related scientific research activities are planned to continue for 6 years.

Other missions, coordinated with and scientifically complementing the vehicles in the libration point orbits, will be launched in the next decade, as well. A set of four spacecraft called CLUSTER will be located in polar Earth orbits at the same time that SOHO is in its libration point orbit. CLUSTER will provide complementary solar-terrestrial measurements from inside the Earth's magnetosphere.[11] A NASA-controlled mission, POLAR, is planned for injection into a northern Earth polar orbit in order to take measurements of the magnetosphere. GEOTAIL, an ISAS-controlled mission, is planned to primarily study the geomagnetic tail. A joint NASA/DoD mission, the Combined Release and Radiation Effects Satellite (CRRES), is planned to be in an Earth orbit in order to investigate the near-Earth plasma sheet and the outer Van Allen belt.[11] Numerous specific missions are also being planned for launch into libration point orbits after the turn of the century. Scientific interest in libration point orbits of various sizes and shapes, tailored to specific missions, will thus continue to increase.

d. Halo Orbits

Three-dimensional, periodic "halo" orbits in the vicinity of the collinear libration points have been studied since the late 1960s. Early work concerning these orbits was motivated by studies related to exploring the far side of the Moon. These studies were completed in support of the planned Apollo 18 lunar exploration mission that was later canceled. Robert Farquhar coined the term "halo" to describe a three-dimensional, periodic orbit near a libration point on the far side of the Moon in the Earth-Moon system.[13] These orbits were designed to be large enough so that the spacecraft would be constantly in view of the Earth and would thus appear as a halo around the Moon.

A communications station in this type of orbit could maintain constant contact between the Earth and a lunar experimentation station on the far side of the Moon.[14]

Interest in these periodic, three-dimensional orbits has continued. Since the late 1960s, a number of researchers have produced approximate analytic, as well as numerically integrated, solutions that represent three-dimensional, periodic halo orbits in the restricted three-body problem; some have also conducted stability studies on many families of such orbits.[15-22] In the CR3BP, precisely periodic halo paths can be constructed, and the orbital symmetry of the constructed trajectory can be fully exploited to facilitate the numerical computations. However, in the ER3BP, orbital construction is more difficult, and halo-type orbits that are not perfectly periodic may result.

An orthographic projection of approximately one revolution of a halo-type orbit in the Sun-Earth ER3BP is depicted in Figure 1-2. This view of the orbit is only one of the three possible orthographic depictions of a three-dimensional orbit, and it is included here for illustrative purposes--the actual orbits used in this research will be fully described in the following chapter. The orbit is generated near the libration point located between the Sun and the Earth. This planar projection is perpendicular to the line between the primaries; thus, it is the view of the orbit as seen when looking toward the Sun from the Earth. Note that the z coordinate represents out-of-plane motion. Since the distance between the Sun and the Earth is approximately 1.5×10^8 kilometers, the z excursion is relatively small but significant. Note also that the maximum y excursion for this halo-type orbit is nearly four times as large as its maximum z excursion.

A recently successful mission in which the spacecraft moved on a halo trajectory about a libration point between the Earth and the Sun has helped spur continuing interest in libration point orbits. On August 12, 1978, a scientific spacecraft named the International Sun-Earth Explorer-3 (ISEE-3) was launched toward a halo orbit near the interior Sun-Earth libration point. It remained in orbit for nearly 4

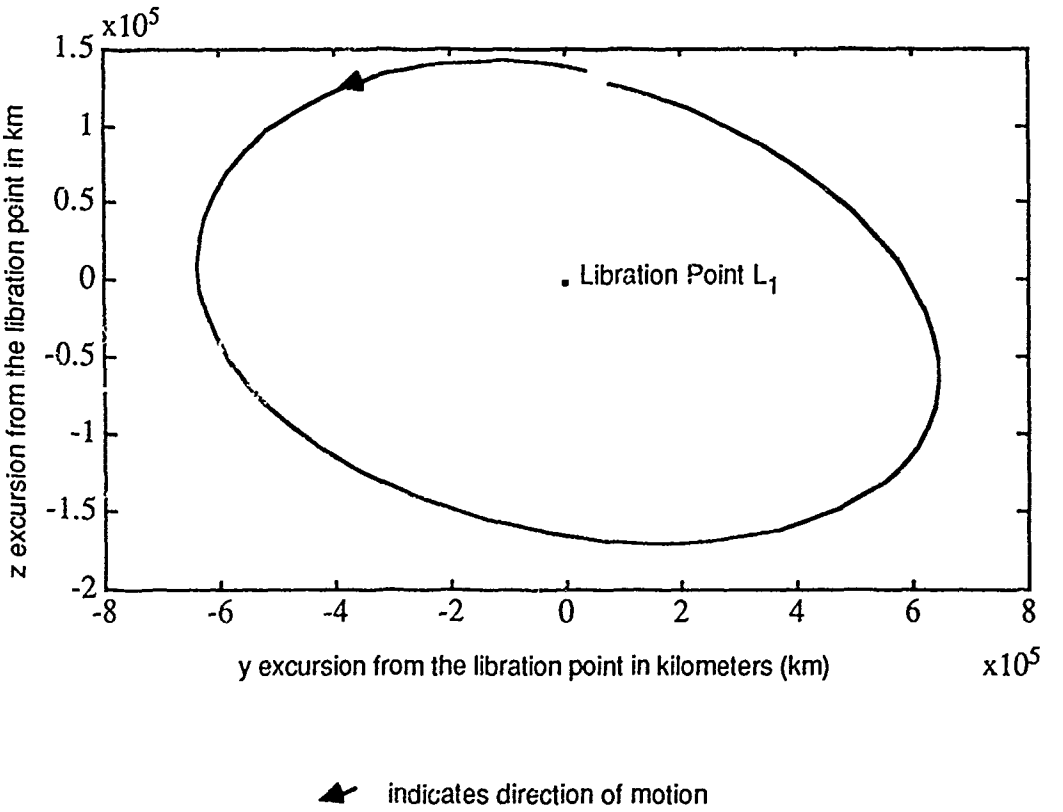

Figure 1-2. An Orthographic Depiction of a Halo-Type Orbit.

years to measure solar wind characteristics and for the study of other solar-induced phenomena such as solar flares upstream of the Earth. Measurements associated with these processes could be made at the interior Lagrange point approximately 1 hour before any disturbance reached the terrestrial environment. Concurrently, the ISEE-1 and ISEE-2 missions measured similar characteristics from Earth orbit in order to complete a comparative study. Future missions planned as part of the upcoming ISTP program are being designed to continue the investigation of the solar-terrestrial environment.[11]

e. Lissajous Orbits

Quasi-periodic orbits near libration points are also currently of great research interest. One orthographic view of several revolutions of a Lissajous orbit constructed near the interior libration point in the Sun-Earth ER3BP is depicted in Figure 1-3. This is the view of the orbit as seen when looking toward the Sun from the Earth. This single view of the three-dimensional Lissajous orbit is included for illustrative purposes and for a comparison with the halo-type orbit depicted in Figure 1-2. Note that the z excursions of the two orbits are comparable; yet, the maximum y excursion of the Lissajous path is only approximately one-fourth that of the halo-type orbit.

The variations in size and shape that a quasi-periodic orbit can exhibit may add valuable flexibility for mission planning. This type of bounded, three-dimensional libration point trajectory is called a Lissajous orbit since specific planar projections of these quasi-periodic trajectories may look like a special type of "Lissajous" curve. Physicist Jules Antoine Lissajous (1822-1880) investigated curves that were generated by compounding simple harmonic motions at right angles, and he delivered a paper on this subject to the Paris Academy of Sciences in 1857. Nathaniel Bowditch of Salem, Massachusetts, had conducted some similar work in 1815. Lissajous curves have a wide variety of shapes that depend on the frequency,

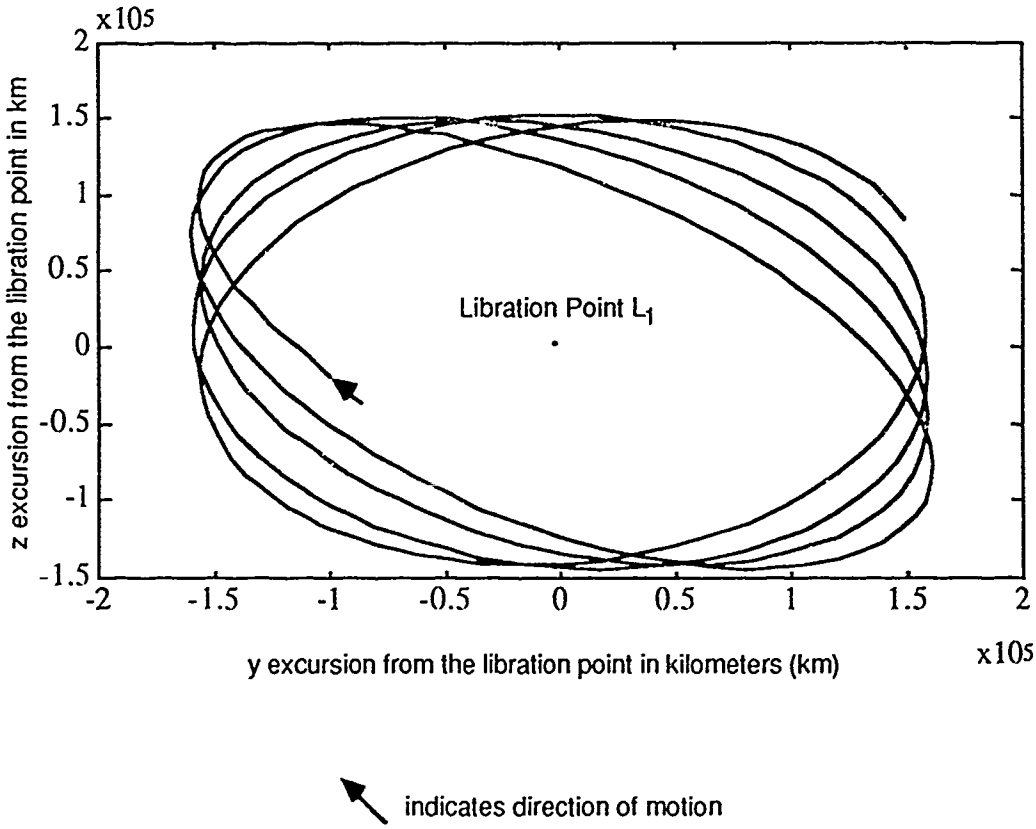

Figure 1-3. An Orthographic Depiction of a Lissajous Orbit.

phase, and amplitude of the orthogonal components of the motion.[23,24] When the in-plane and the (orthogonal) out-of-plane frequencies of the linearized motion are nearly (but not) equal, the resulting path is typically called a Lissajous trajectory.

A method to generate approximations for this type of quasi-periodic orbital path was developed analytically by Farquhar and Kamel in 1973.[15] They derived a third-order approximate analytic solution for a translunar libration point orbit in the Earth-Moon ER3BP that also included solar gravity perturbations. In 1975, Richardson and Cary then developed a fourth-order analytic Lissajous approximation in the Sun-Earth+Moon barycenter system.[25] The notation "Earth+Moon" indicates that the Earth and the Moon are treated as one body with mass center at the Earth-Moon barycenter. In consideration of the lunar perturbation, Farquhar has shown that the accuracy of solutions in the Sun-Earth CR3BP can be enhanced if the collinear libration points are defined along the line between the Sun and the center of mass of the Earth and the Moon.[17] Since 1975, a few researchers have considered methods to numerically generate Lissajous trajectories, but the lack of periodicity of a Lissajous path complicates numerical construction of bounded trajectories. Howell and Pernicka have developed a numerical technique for determination of three-dimensional, bounded Lissajous trajectories of arbitrary size and duration.[12,26-30]

C. Overview

This next chapter considers the research results and briefly discusses the following topics: coordinate systems, equations of motion, locations of the five Lagrange points, linearization of the equations in order to compute the state transition matrix, and construction of bounded orbits near the equilibrium points. Follow-on studies (not presented here) can then be used to conduct tracking and control scheme simulations, incorporating the solar radiation pressure force, for a spacecraft in such an orbit.

CHAPTER 2: RESULTS

In this chapter, the elliptic restricted three-body problem and the associated coordinate systems are reviewed; the equations of motion for an infinitesimal mass moving in the gravity fields of two massive bodies are then derived. Locations of the libration points are discussed, and then the computation of the state transition matrix and the construction of bounded nominal orbits near the collinear Lagrange points are summarized.

A. Elliptic Restricted Three-Body Problem

The elliptic restricted three-body problem is a simplification of the general problem of three bodies. In the general three-body problem, each of the three bodies is assumed to be a particle of finite mass and, thus, exerts an influence on the motion of each of the other bodies. Neither the general nor the restricted problem of three bodies has a general closed-form solution. However, when problem simplifications are made, particular solutions can be determined. If the mass of one of the bodies is restricted to be infinitesimal, such that it does not affect the motion of the other two massive bodies (primaries), the restricted three-body model results. The primaries are assumed to be in known elliptic (ER3BP) or circular (CR3BP) orbits about their common mass center (barycenter). The problem can then be completely described by a single second-order vector differential equation with variables appropriately defined for a specified coordinate frame.

B. Coordinate Systems

The two standard coordinate systems used in the analysis of this problem have a common origin at the center of mass (barycenter) of the primaries. Primaries with masses m_1 and m_2 such that $m_1 \geq m_2$ are assumed here, although this distinction is arbitrary. The infinitesimal mass is denoted as m_3. These masses (m_1, m_2, m_3) correspond to particles situated at points P_1, P_2, and P_3, respectively. The barycenter is denoted as "B," and the resulting arrangement is shown in Figure 2-1. The rotating coordinate system is defined as $x_R y_R z_R$, and the inertial system is identified as $x_I y_I z_I$. Note that both coordinate systems are right-handed, and the x and y axes for both systems are in the plane of motion of the primaries. The x_I axis is, of course, assumed to be oriented in some fixed direction; in this specific formulation of the problem, it is assumed to be parallel to a vector defined with a base point at the Sun and directed toward periapsis of the Earth's orbit. The rotating x_R axis is defined along the line that joins the primaries and is directed from the larger toward the smaller primary. The z axes are coincident and are directed parallel to the primary system angular momentum vector. The y_R axis completes the right-handed $x_R y_R z_R$ system.

C. Equations of Motion

Newtonian mechanics are used to formulate the equations of motion for m_3 (the spacecraft) relative to B as observed in the inertial reference frame. The sum of the forces on m_3 resulting from both the gravity fields of masses m_1 (the Sun) and m_2 (the Earth-Moon

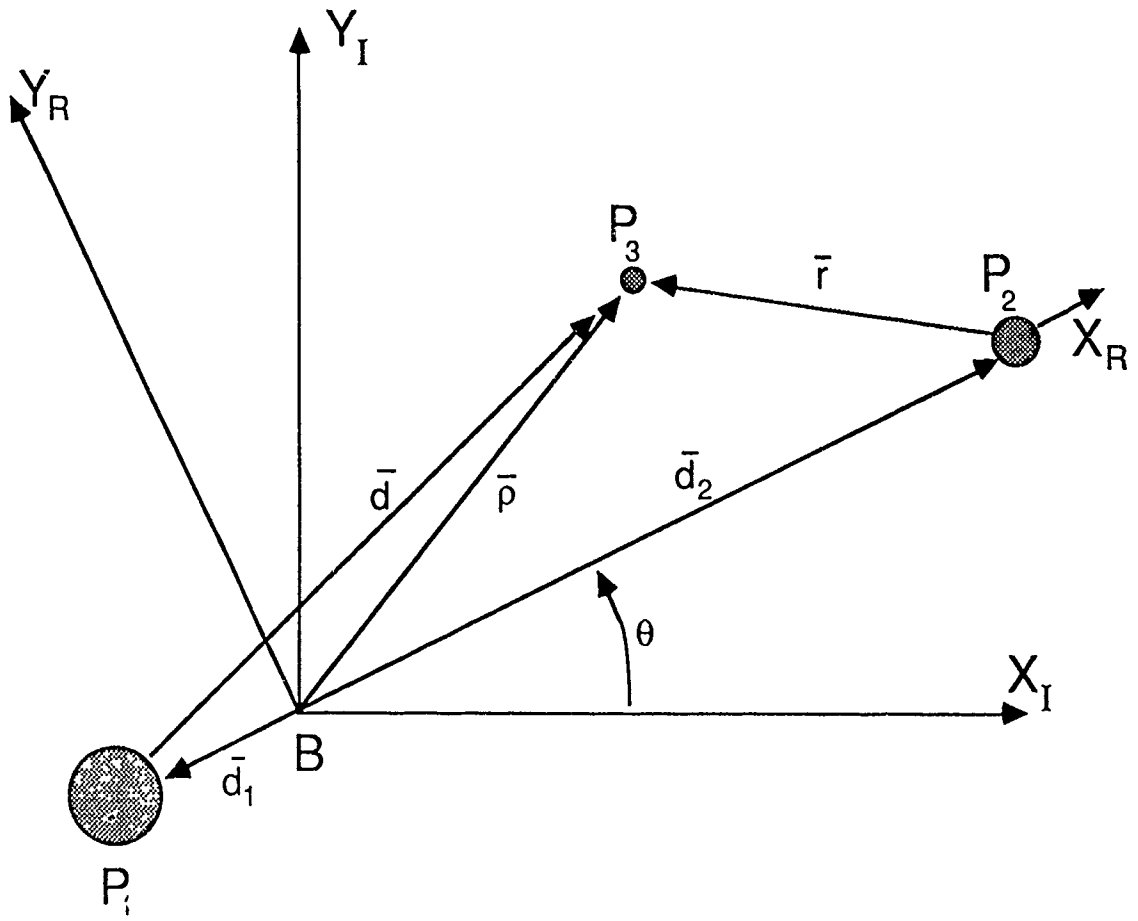

Figure 2-1. Coordinate Systems With Barycenter Origin.

barycenter) and from the solar radiation pressure can be used to produce the following second-order vector differential equation:

$$\bar{\rho}'' = - G \left(\frac{m_1}{d^3}\right) \bar{d} - G \left(\frac{m_2}{r^3}\right) \bar{r} + \left(\frac{kS}{d^3}\right) \bar{d}. \qquad (2\text{-}1)$$

The overbar denotes a vector, and primes indicate differentiation with respect to dimensional time. All quantities are dimensional, as appropriate, and the quantity "G" is the universal gravitiational constant. The scalars "d" and "r" in equation (2-1) denote the magnitudes of the vectors $\bar{d}$ and $\bar{r}$, respectively, as depicted in Figure 2-1. The dimensionless scalar "k" is the solar reflectivity constant, and "S" is the solar radiation pressure constant. The formulation of the solar radiation force model and the values for the solar radiation constants are derived from previous work by Bell.[31] The numerical values for these constants are selected from characteristic data for ISEE-3; however, they should also approximately model a vehicle such as SOHO in the International Solar-Terrestrial Physics Program:

$$S = \frac{A\, S_0\, r_0^2}{c\, m_3}, \qquad (2\text{-}2)$$

where k = 1.2561, S_0= 1352.098 kg/sec^3, r_0 = 1.4959787x10^8 km, c = the speed of light = 2.998x10^8 m/sec, A = surface area of the spacecraft's sun-facing side = 3.55 m^2, and m_3 = mass of the spacecraft = 435 kg. The constant S_0 is the solar light flux measured at one astronomical unit (A.U.), and r_0 is the nominal distance associated with the measurement of the solar flux S_0.[31] The value of A, also termed the effective cross-sectional area of the spacecraft, is considered to be constant in this work. The constant k is a material parameter

dependent on the absorptivity of the spacecraft surface and is generally confined to a range of $0 \leq k \leq 2.0$.[31]

The position vector $\bar{\rho}$ is written in rotating components as

$$\bar{\rho} = x\,\hat{x}_R + y\,\hat{y}_R + z\,\hat{z}_R \tag{2-3}$$

where $\hat{x}_R, \hat{y}_R, \hat{z}_R$ are unit vectors. The velocity and the acceleration of the spacecraft (particle P_3 with mass m_3) relative to the barycenter B as observed in the inertial reference frame can then be derived by using the basic kinematic expressions

$$\bar{\rho}' = \bar{\rho}'^{I} = \bar{\rho}'^{R} + {}^{I}\bar{\omega}^{R} \times \bar{\rho}, \tag{2-4}$$

and

$$\bar{\rho}'' = \bar{\rho}''^{IR} + {}^{I}\bar{\omega}^{R} \times \bar{\rho}' \tag{2-5}$$

where the superscript "I" denotes the inertial reference frame, the superscript "R" indicates the rotating reference frame, $\bar{\rho}''^{IR}$ denotes the time derivative of $\bar{\rho}'^{I}$ in equation (2-4) taken with respect to the rotating frame, and ${}^{I}\bar{\omega}^{R}$ is the angular velocity of the rotating reference frame relative to the inertial frame. The symbol "x" indicates a vector product.

Assuming an elliptic primary orbit and a known time of periapsis passage for the primary orbit, two-body orbital mechanics can be used to determine the position of P_2 in its orbit at any given time. In the standard two-body problem, the angular displacement of $\bar{d}_2$ from periapsis is defined by the angle θ as depicted in Figure 2-1. Clearly, the angle θ in this particular formulation is also the angular displacement of the rotating reference frame relative to the fixed inertial system.

Hence, the angular velocity of the rotating frame relative to the inertial direction is written

$$\bar{\omega}^{I-R} = \theta' \hat{Z}. \tag{2-6}$$

Using equations (2-3) and (2-6) in equation (2-4), an expression for the velocity of P_3 can be obtained:

$$\bar{\rho}' = \bar{\rho}'^{I} = (x' - \theta' y)\,\hat{x}_R + (y' + \theta' x)\,\hat{y}_R + z'\hat{z}_R. \tag{2-7}$$

Then, using equations (2-6) and (2-7) in equation (2-5), the following kinematic expression for $\bar{\rho}''$ can be derived:

$$\bar{\rho}'' = (x''-\theta'' y-2\theta' y'-\theta'^2 x)\hat{x}_R+(y''+\theta'' x+2\theta' x'-\theta'^2 y)\hat{y}_R+z''\hat{z}_R. \tag{2-8}$$

Notice that equation (2-8) includes terms with the angular velocity, $\theta'(t)$, and angular acceleration, $\theta''(t)$, of the rotating reference frame with respect to the inertial frame. By using known elliptic orbital elements, readily computed expressions for θ' and θ'' can be found. For instance, the magnitude of the specific angular momentum vector can be computed by using a vector equation that includes θ':

$$\bar{h} = h\,\hat{z} = \bar{R} \times \bar{v} = R\,\hat{x}_R \times (R'\hat{x}_R + R\theta'\hat{y}_R) = R^2\theta'\hat{z} \tag{2-9}$$

where the vector $\bar{v}$ is the orbital velocity of the smaller primary, P_2, in its elliptic orbit, as observed in the fixed frame. For the elliptic two-body orbit, the varying distance R between the primaries

is given by

$$R = R(t) = a\ (1 - e\ \cos(E)), \tag{2-10}$$

where "e" is the eccentricity, "E" is the eccentric anomaly, and "a" is the semi-major axis of the primary orbit.

For any orbit, the semi-latus rectum, p, is expressed

$$p = h^2 / G\ (m_1 + m_2). \tag{2-11}$$

For any conic orbit that is not a parabolic path, p can also be written

$$p = a(1 - e)^2 = a(1-e)(1+e). \tag{2-12}$$

Using equations (2-11) and (2-12), an expression for h can be found:

$$h = \sqrt{a(1-e)(1+e)}\ \sqrt{G(m_1 + m_2)}. \tag{2-13}$$

Hence, using equations (2-9), (2-10), and (2-13), the angular rate, θ', can be computed as

$$\theta' = \frac{h}{R^2} = \frac{\sqrt{a(1-e)(1+e)}\ \sqrt{G(m_1+m_2)}}{a^2\ (1 - e\ \cos(E))^2}\ . \tag{2-14}$$

Equation (2-14) includes, however, the angle "E" that varies with time. Therefore, the expression for the angular acceleration, θ'', will

necessarily include E', for which a relationship in terms of known orbital elements must be found. An equation that relates the eccentric anomaly and the time since periapsis passage is given as

$$t - t_p = \left(\sqrt{a^3/G(m_1 + m_2)}\right) (E - e \sin (E)) \qquad (2\text{-}15)$$

where t_p is the time of periapsis passage. The quantity $\sqrt{G(m_1 + m_2)/a^3}$ is denoted as the mean motion, n_{mean} ; that is,

$$n_{mean} = \sqrt{G(m_1 + m_2)/a^3}, \qquad (2\text{-}16)$$

and equation (2-15) can be rewritten as

$$n_{mean}(t - t_p) = (E - e \sin (E)). \qquad (2\text{-}17)$$

Equations (2-15) or (2-17) can be used to derive a mathematical relationship involving the time derivative of E and other known orbital elements. Equation (2-17) will later prove to be quite useful in determining the angle E if both the time, t, and the time of periapsis passage, t_p, are known. Differentiating equation (2-15) with respect to time produces

$$E' = \frac{\sqrt{G(m_1+m_2)/a}}{a(1-e \cos(E))}. \qquad (2\text{-}18)$$

Taking the time derivative of equation (2-14) and using equation (2-18), the angular acceleration of the rotating reference frame relative to the inertial frame can be computed as

$$\theta'' = \frac{-2G(m_1+m_2)\sqrt{(1-e)(1+e)}\ e\ \sin(E)}{a^3(1 - e\ \cos(E))^4}. \qquad (2\text{-}19)$$

Then equations (2-1), (2-2), (2-8), (2-14), (2-15), and (2-19) comprise the governing set of equations for motion of the infinitesimal mass within the force environment of the Earth+Moon (m_2) and the Sun (m_1), including the solar radiation pressure force. Note that equation (2-15) is listed here. Equation (2-15), or its mathematical equivalent (2-17), known as Kepler's equation, is used to compute the angle E when the time since periapsis passage is known. Of a number of different procedures, Newton's method for finding the zeros of a function proves adequate for this purpose in this work; that is, given t_p and time t, the correct value of the angle E must be computed. Newton's method is iterative and, in this work, finds the zero of a function defined as

$$f(E) = n_{mean}(t - t_p) - E + e\ \sin(E). \qquad (2\text{-}20)$$

The algorithm reduces to finding iterative solutions based on the equation[26]

$$E_n = E_{n-1} - \frac{n_{mean}(t - t_p) - E_{n-1} + e\ \sin(E_{n-1})}{-1 + e\ \cos(E_{n-1})}. \qquad (2\text{-}21)$$

The iteration process using equation (2-21) is defined as complete when the condition $|f(E_{n-1})| \leq 10^{-12}$ is satisfied. (The symbol "| |", of course, indicates that the absolute value is to be taken.) Thus, by using equation (2-21), the value of the eccentric anomaly, E, at any time, t, relative to the time of periapsis passage, t_p, can be calculated and then used in equations (2-14) and (2-19) to determine θ' and θ''.

Three scalar equations of motion for P_3 can be derived using the dimensional equations (2-1), (2-2), (2-8), (2-14), and (2-19); however, for convenience, the following scaling factors are typically introduced:

(1) The sum of the masses of the primaries equals one mass unit. ($m_1 + m_2 = 1$ unit of mass)

(2) The mean distance between the primaries equals one unit of distance. (a = 1 unit of distance)

(3) The universal gravitational constant is equal to one unit by proper choice of characteristic time. (characteristic time = $1/n_{mean}$; thus G = 1 unit)

The dimensional equations of motion can be simplified and scaled by introducing the characteristic quantities defined above and by introducing the nondimensional mass ratio μ, "psuedo-potential" U, and the scaled solar radiation constant s:

$$\mu = \frac{m_2}{m_1 + m_2} \tag{2-22}$$

and

$$U = \frac{(1-\mu)}{d} + \frac{\mu}{r} + \frac{1}{2}\dot{\theta}^2(x^2 + y^2) - \frac{k\,s}{d} \tag{2-23}$$

where the dot denotes the derivative with respect to nondimensional time. The scaled solar radiation constant, s, is derived from the dimensional radiation constant denoted as S in equation (2-2) and, by using the characteristic quantities described above, its value is calculated as $s = 6.206597029461384 \times 10^{-6}$ nondimensional units. Then, the vector magnitudes, "d" and "r," are written in terms of scaled quantities as:

$$d = [(x + \mu R)^2 + y^2 + z^2]^{1/2}, \tag{2-24}$$

$$r = [(x - R + \mu R)^2 + y^2 + z^2]^{1/2}. \tag{2-25}$$

The three scalar second-order differential equations that result can be written in terms of characteristic quantities as

$$\ddot{x} - 2\dot{\theta}\dot{y} = \frac{\partial U}{\partial x} + \ddot{\theta} y = U_x + \ddot{\theta} y, \tag{2-26}$$

$$\ddot{y} + 2\dot{\theta}\dot{x} = \frac{\partial U}{\partial y} - \ddot{\theta} x = U_y - \ddot{\theta} x, \tag{2-27}$$

$$\ddot{z} = \frac{\partial U}{\partial z} = U_z, \tag{2-28}$$

where

$$U_x = -\frac{(1-\mu)(x+R\mu)}{d^3} - \frac{\mu(x-R+\mu R)}{r^3} + \frac{ks(x+R\mu)}{d^3} + \dot{\theta}^2 x \ , \qquad (2\text{-}29)$$

$$U_y = -\frac{(1-\mu)y}{d^3} - \frac{\mu y}{r^3} + \frac{ksy}{d^3} + \dot{\theta}^2 y \ , \qquad (2\text{-}30)$$

$$U_z = -\frac{(1-\mu)z}{d^3} - \frac{\mu z}{r^3} + \frac{ksz}{d^3} \ . \qquad (2\text{-}31)$$

The scaled equations for the angular velocity and angular acceleration of the rotating frame relative to the inertial frame also simplify:

$$\dot{\theta} = \frac{h}{r^2} = \frac{\sqrt{(1-e)(1+e)}}{(1 - e\cos(E))^2}, \qquad (2\text{-}32)$$

$$\ddot{\theta} = \frac{-2\sqrt{(1-e)(1+e)}\ e\sin(E)}{(1 - e\cos(E))^4}. \qquad (2\text{-}33)$$

If the primaries are assumed to be moving in a circular orbit, then $\ddot{\theta} = 0$, $R = \dot{\theta} = 1$, and equations (2-26), (2-27), (2-28) reduce to three scalar equations in the simplified form:

$$\ddot{x} - 2\dot{y} = \frac{\partial U}{\partial x} = U_x, \tag{2-34}$$

$$\ddot{y} + 2\dot{x} = \frac{\partial U}{\partial y} = U_y, \tag{2-35}$$

$$\ddot{z} = \frac{\partial U}{\partial z} = U_z, \tag{2-36}$$

where

$$U_x = -\frac{(1-\mu)(x+\mu)}{d^3} - \frac{\mu(x-1+\mu)}{r^3} + \frac{ks(x+\mu)}{d^3} + x, \tag{2-37}$$

$$U_y = -\frac{(1-\mu)y}{d^3} - \frac{\mu y}{r^3} + \frac{ksy}{d^3} + y, \tag{2-38}$$

$$U_z = -\frac{(1-\mu)z}{d^3} - \frac{\mu z}{r^3} + \frac{ksz}{d^3}. \tag{2-39}$$

The system of equations (2-34), (2-35), and (2-36) admits an integral of the motion that was originally found by Jacobi:

$$J = 2U - \dot{x}^2 - \dot{y}^2 - \dot{z}^2 = \text{constant}. \tag{2-40}$$

In addition to offering special insight into the CR3BP, Jacobi's constant can be used as a check during numerical integration of the equations of motion; however, it is not a constant in the ER3BP.

The scalar equations (2-26), (2-27), and (2-28) corresponding to the elliptic restricted problem or equations (2-34), (2-35), and (2-36) derived for the circular restricted problem can be used to locate the five libration points in the rotating reference frame

D. Locations of the Lagrangian Points

By using scalar equations (2-34), (2-35), and (2-36) for motion in the CR3BP, the locations of the stationary equilibrium points can be determined. Equations (2-26), (2-27), and (2-28) can be used to determine ratios of distances that are constant in the ER3BP. These ratios are related to the locations of libration points that have been defined in the ER3BP and that "pulsate" with respect to the rotating reference frame as the distance between the primaries varies with time.

1. The CR3BP

In the CR3BP, the five libration points are equilibrium points and are stationary with respect to the rotating coordinate frame, that is, they are locations at which the forces on the third body sum to zero. The arrangement of points and the corresponding nondimensional distances are depicted in Figure 2-2. Note that three of the libration points (L_1, L_2, L_3) are collinear with the primaries; one collinear point (L_1) is interior to the primaries. The remaining two points (L_4 and L_5) are located at the vertices of two equilateral triangles that are in the plane of primary rotation and that have a common base between the primaries.

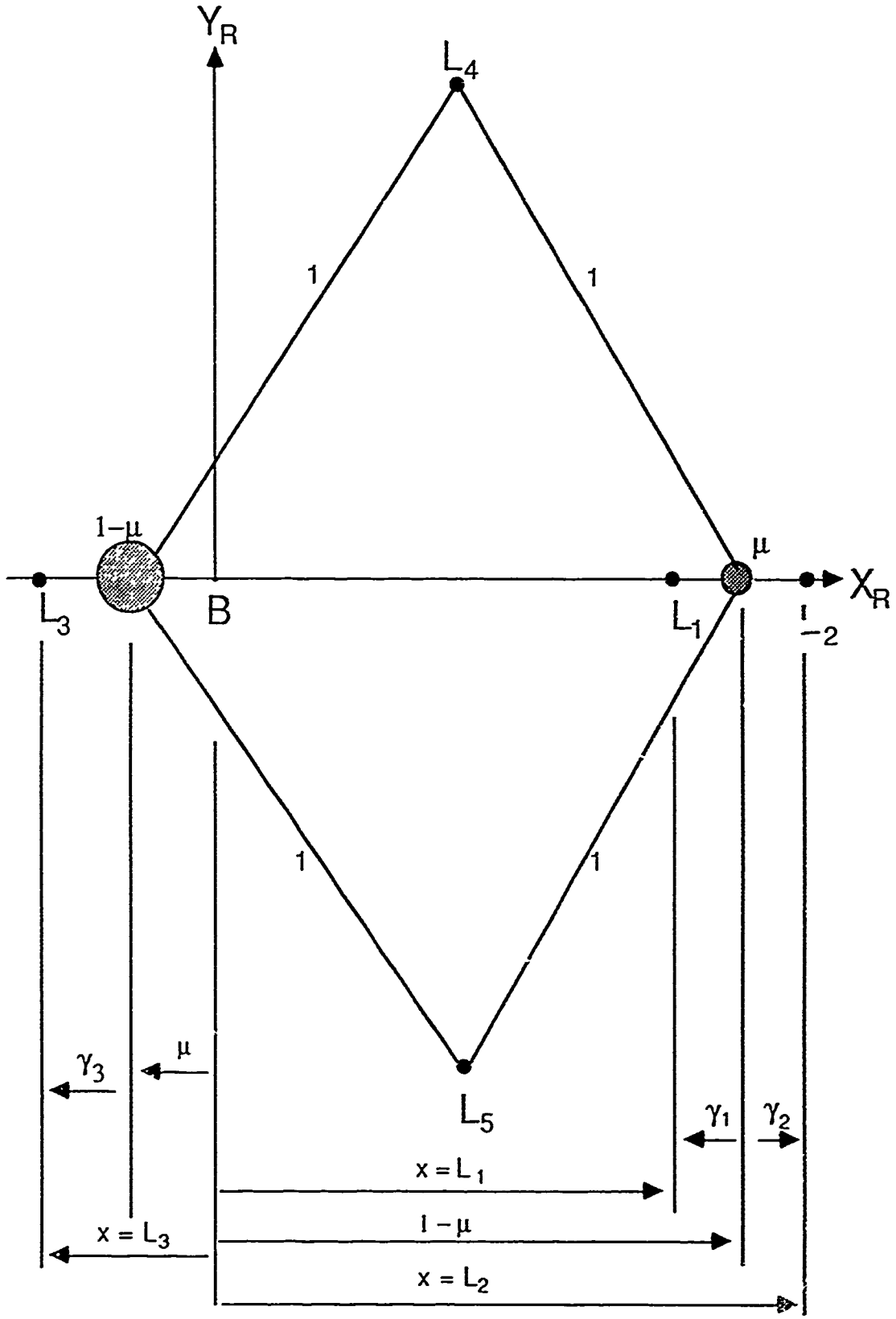

Figure 2-2. Lagrange Point Locations in the Scaled CR3BP.

In the CR3BP, the libration points are stationary in the rotating coordinate frame. Stationary points are defined as points at which the relative velocity and acceleration are zero, such that

$$\dot{x} = \dot{y} = \dot{z} = \ddot{x} = \ddot{y} = \ddot{z} = 0. \tag{2-41}$$

Using equations (2-41) in equations (2-34) through (2-39), the useful conditions $U_x = U_y = U_z = 0$ are found. The three collinear libration points can be readily located by further noting that $y = z = 0$ for the points located on the rotating x_R axis.

Then, the remaining equation that allows conditions on the coordinate x to be found is (2-37). For the collinear libration points, equation (2-37) then reduces to

$$U_x = 0 = -\frac{(1-\mu)(x+\mu)}{d^3} - \frac{\mu(x-(1-\mu))}{r^3} + \frac{ks(x+\mu)}{d^3} + x. \tag{2-42}$$

By substituting the appropriate coordinates into equation (2-42) for each of the three collinear Lagrange points, the locations of the three points can then be individually determined.

However, before deriving the equations that are used to locate each of the libration points, the values of the constants used to solve equation (2-42) are noted here. The value of μ used in this work is $3.0404234945077 \times 10^{-6}$ (consistent with the Sun/Earth+Moon system). The characteristic distance equals the semi-major axis of the primary orbit; that is, $a = 1.4959787066 \times 10^{8}$ kilometers. When the solar radiation pressure force is included in the model, the values of the nondimensional constants include the values of $k = 1.2561$ and $s = 6.206597029461384 \times 10^{-6}$ scaled units. Also, note that when the constants "k" or "s" are defined to be zero, equation (2-42) reduces to the equation derived for the CR3BP without the solar radiation force; it may be useful and interesting to compare the positions of the

collinear points with and without solar radiation pressure forces included in the model. First, however, it is appropriate to briefly discuss the selection of the parameter values used in this solar radiation pressure model.

The values chosen for computation of the solar radiation pressure force deserve special discussion here because they have a minor, yet important, impact on several of the numerical results. The computation of the solar radiation pressure constant S is described in equation (2-2). (The scaled solar radiation pressure constant is denoted as s.) The values of the parameters used in that equation are selected from research by Bell[31] using post-flight data for the ISEE-3 mission near Lagrange point L_1. Certainly, many factors can affect the accuracy of this solar radiation pressure approximation. The orientation of the spacecraft may alter the area of its Sun-facing side (the variable A in equation (2-2)), and the position of the spacecraft at a libration point other than L_1 may require modification of at least the variable r_0 in equation (2-2).

The value 1.2561 chosen for the solar reflectivity constant k conforms with other research[57,59,80] concerning ISEE-3; yet, it too is clearly an approximation. The values used in these works for ISEE-3 include estimated values for k of 1.20 and 1.30; also, using actual flight data for ISEE-3, the constant k was at times treated as a solved-for parameter. While its value varied widely during flight, some of the solved-for values at various epochs were 1.258, 1.261, and 1.260.[59,80] (It may be interesting to note that the reflectivity properties of any spacecraft surface may change with age, that is, with time on station, due in part to possible particulate impacts and solar radiation.) Early work by Bell used a k value of 1.2561; this is the nominal value of k used to generate the reference trajectories for the orbit determination error analysis and station-keeping studies in this work. More recent work by Bell includes a k value of 1.20. The results of using this smaller value of k when determining the locations of the Lagrange points will be included in the next few paragraphs.

The positive constant γ_1 is the distance between the smaller primary mass and the libration point L_1 as depicted in Figure 2-2. For libration point L_1, $x = L_1 = 1 - \mu - \gamma_1$ (see Figure 2-2), and the following quintic is derived from equation (2-42):

$$\gamma_1^5 - (3-\mu)\gamma_1^4 + (3-2\mu)\gamma_1^3 - (\mu+ks)\gamma_1^2 + 2\mu\gamma_1 - \mu = 0. \qquad (2\text{-}43)$$

The nondimensional position of L_1 relative to P_2 in the CR3BP can be determined by finding the single real root of equation (2-43), which for this problem with k = 1.2651 has a value γ_1 = .01001184941667781. When solar radiation pressure is not included, the position of L_1 is determined by the value γ_1 = .01001097733285880. Hence, the position of Lagrange point L_1 moves approximately 130.46188 kilometers closer to the Sun (m_1 at P_1) when solar radiation pressure forces are included in the circular model. Bell[31] computes a value of 124.60 kilometers for the change in the position of L_1 if the solar radiation pressure force with k = 1.20 is included.

For libration point L_2, $x = L_2 = 1 - \mu + \gamma_2$ (see Figure 2-2), and the following quintic is derived from equation (2-42):

$$\gamma_2^5 + (3-\mu)\gamma_2^4 + (3-2\mu)\gamma_2^3 - (\mu-ks)\gamma_2^2 - 2\mu\gamma_2 - \mu = 0. \qquad (2\text{-}44)$$

When solar radiation pressure forces with k = 1.2561 are included in the model, the location of Lagrange point L_2 is defined by the nondimensional value γ_2 = .01007738021243130. When solar radiation pressure is not included, the position of Lagrange point L_2 is calculated as γ_2 = .01007824054648482. Hence, the location of L_2 in the CR3BP moves approximately 128.70414 kilometers closer to the Sun when solar radiation pressure forces with k = 1.2561 are included in

the model. Bell[31] computes a value of 122.90 kilometers for the change in the position of L_2 if the solar radiation pressure force with k = 1.20 is incorporated. (Note that solar radiation pressure forces may not actually influence a spacecraft in an orbit that remains on the dark side of the Earth, that is, in the Earth's shadow. In fact, the size and shape of the orbit will be reflected in the magnitude of the solar radiation force on the spacecraft near L_2.)

For libration point L_3, $x = L_3 = -\mu - \gamma_3$ (see Figure 2-2), and the following quintic is derived from (2-42):

$$\gamma_3^5+(2+\mu)\gamma_3^4+(1+2\mu)\gamma_3^3-(1-\mu-ks)\gamma_3^2-(2-2\mu-2ks)\gamma_3-(1-\mu-ks) = 0. \quad (2-45)$$

When solar radiation pressure with k = 1.2561 is included in the force model, the location of Lagrange point L_3 is determined as γ_3 = .9999956277060894 in nondimensional units. Without solar radiation pressure, the location of L_3 is calculated as γ_3 = .9999982264196291. Hence, the location of L_3 in the CR3BP moves approximately 388.762012 kilometers closer to the Sun when solar radiation pressure forces are included in the model.

The addition of the solar radiation pressure force then causes the location of the Lagrange point to move closer to the Sun for all three collinear libration points. It would also be logical to question how solar radiation pressure forces affect the locations of the remaining two Lagrange points. The existence and locations of the triangular Lagrange points when solar radiation pressure forces are included may be valuable, but such an investigation is not part of this effort. The focus here now turns to the locations of the Lagrange points in the ER3BP, which is the dynamic model used for this work.

2. The ER3BP

Five libration points also exist in the ER3BP, but they are not stationary relative to the rotating frame; rather, the collinear points pulsate along the x_R axis, and the triangular points pulsate relative to both the x_R and the y_R axes as the distance between the primaries varies with time. The equilibrium solutions can be located by using equations (2-26) through (2-31) to find ratios of certain distances that are, in fact, constant in the problem. The collinear libration points in the ER3BP can be found by assuming $\dot{x} \neq 0$, $x \neq 0$, and $\dot{y} = \ddot{y} = \dot{z} = \ddot{z} = y = z = 0$.

With these restrictions on the coordinates of the collinear points, equation (2-27) reduces to

$$2\,\dot{\theta}\,\dot{x} + \ddot{\theta}\,x = 0. \tag{2-48}$$

Also, equations (2-26) and (2-29) combine to produce

$$\ddot{x} = -\frac{(1-\mu)(x+R\mu)}{d^3} - \frac{\mu(x-R+\mu R)}{r^3} + \frac{ks(x+R\mu)}{d^3} + \dot{\theta}^2 x, \tag{2-49}$$

where

$$d = \left| x + R\mu \right|, \tag{2-50}$$

$$r = \left| x - R + \mu R \right|, \tag{2-51}$$

$$R = 1 - e\cos(E). \tag{2-52}$$

Equations (2-48) and (2-49) can be combined to provide one equation written in terms of the coordinate, x, of a particular

collinear Lagrange point. Solving for $\dot{x}$ in equation (2-48) results in

$$\dot{x} = \frac{-\ddot{\theta}\, x}{2\,\dot{\theta}}. \tag{2-53}$$

Expressions for $\ddot{\theta}$ and $\dot{\theta}$ must be substituted into equation (2-53). Using equations (2-32), (2-33), and (2-52), equation (2-53) simplifies to

$$\dot{x} = \frac{e\,\sin(E)\,x}{(1-e\,\cos(E))^2} = \frac{e\,\sin(E)\,x}{R^2}. \tag{2-54}$$

The derivative of equation (2-53) with respect to nondimensional time produces the equation

$$\ddot{x} = \frac{e\,\cos(E) - e^2}{R^3}\,\frac{x}{R}, \tag{2-55}$$

for which the scaled version of equation (2-18), that is

$$\dot{E} = \frac{1}{R}, \tag{2-56}$$

is required.

Using equations (2-32) and (2-55) in equation (2-49), the term $(\ddot{x} - \dot{\theta}^2 x)$ reduces to

$$(\ddot{x} - \dot{\theta}^2 x) = \frac{x}{R}\,\frac{-1}{R^2}. \qquad (2\text{-}57)$$

Finally, using equation (2-57) in equation (2-49), an expression for the x coordinate associated with any of the three collinear Lagrange points in the ER3BP can be derived:

$$\frac{x}{R}\, d^3 r^3 + (\mu-1)\left(\frac{x}{R} + \mu\right) r^3 - \mu\left(\frac{x}{R} - (2-\mu)\right) d^3 + ks\left(\frac{x}{R} + \mu\right) r^3 = 0. \qquad (2\text{-}58)$$

Expressions for x as a function of γ_1 (corresponding to each collinear libration point) can then be substituted into (2-58) to find numerical values for γ_1, γ_2, and γ_3. For the ER3BP, these expressions are

$$x = L_1 = R\,(\,1 - \mu - \gamma_1), \qquad (2\text{-}59)$$

$$x = L_2 = R\,(\,1 - \mu + \gamma_2), \qquad (2\text{-}60)$$

$$x = L_3 = R\,(\,-\mu - \gamma_3\,). \qquad (2\text{-}61)$$

The relative locations of the Lagrange points in the ER3BP are depicted in Figure 2-3.

When equation (2-59), (2-60), or (2-61) is substituted into equation (2-58), equations (2-43), (2-44), or (2-45), respectively, result. Therefore, the relative positions of the collinear libration points can be calculated from the same three quintics that were solved in finding the locations of the collinear points in the CR3BP. The locations of the three points can then be calculated at any time by

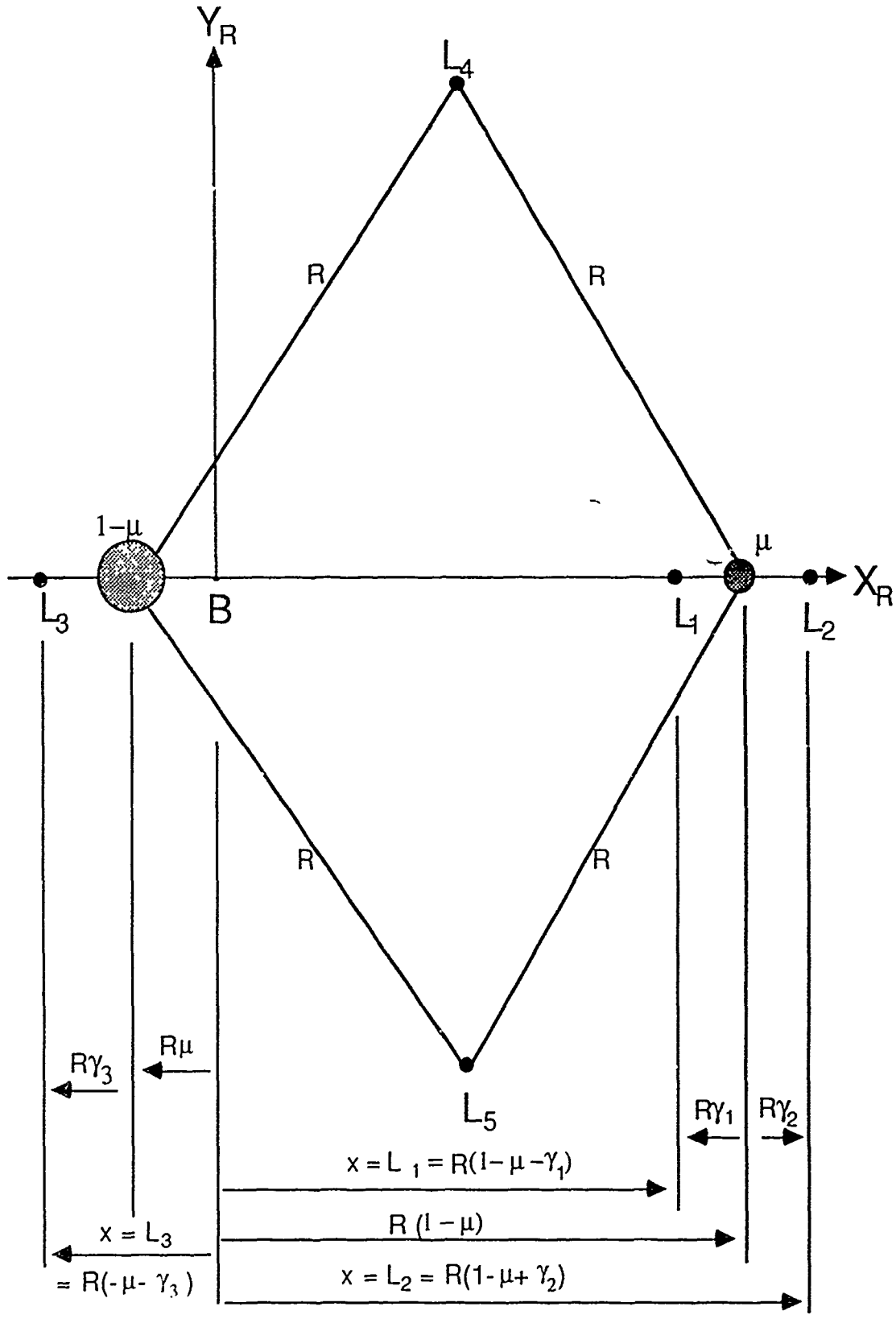

Figure 2-3. Lagrange Point Locations in the Scaled ER3BP.

substituting the appropriate numerical values of γ_1, γ_2, and γ_3 into equations (2-59), (2-60), and (2-61), respectively. Although γ_i are constants, the locations for the collinear points on the rotating x axis vary with time because R(t) is time-varying. The value of e used in these calculations is .01671173051.

For this work, equation (2-59) is used to determine the position of L_1 relative to the barycenter, B; it is also used to transform the numerically integrated data from rotating coordinates with origin at the libration point to rotating coordinates centered at the barycenter.

E. State Transition Matrix

For determination of an acceptable nominal trajectory, as well as orbit determination error analysis investigations and station-keeping studies, it is required that the state transition matrix be available at predetermined but varying time intervals along the nominal path. The transition matrix is derived in connection with a linearizing analysis.

The equations of motion for the infinitesimal mass in the ER3BP can be linearized about a reference trajectory (nominal path) that is a solution of the differential equations. The states, three position and three velocity, and the state vector $\bar{x}$ are defined as

$$x_1 = x,\ x_2 = y,\ x_3 = z\ ,\ x_4 = \dot{x},\ x_5 = \dot{y},\ x_6 = \dot{z}, \tag{2-62}$$

and

$$\bar{x} = [x_1,\ x_2,\ x_3,\ x_4,\ x_5,\ x_6]^T. \tag{2-63}$$

The reference trajectory is defined as $\bar{x}_{REF}$. Therefore, using a Taylor's series approach, the expansion about the reference path is

written in the form of the first-order variational equation

$$\frac{d}{dt}(\tilde{x}) = \dot{\tilde{x}} = A(t)\,\tilde{x} \tag{2-64}$$

where $\tilde{x} = \bar{x} - \bar{x}_{REF}$ is understood to be the vector of residuals relative to the nominal solution, and the matrix A(t) contains the first-order terms in the Taylor's series expansion of the equations of motion about the nominal or reference solution of interest.

Using equations (2-26) through (2-31), A(t) can be expressed as

$$A(t) = \begin{bmatrix} 0 & I \\ U_{rr}+\ddot{\theta}\Omega & 2\dot{\theta}\Omega \end{bmatrix} \tag{2-65}$$

where all four submatrices are dimension 3x3 and

$$U_{rr} = \begin{bmatrix} U_{xx} & U_{xy} & U_{xz} \\ U_{yx} & U_{yy} & U_{yz} \\ U_{zx} & U_{zy} & U_{zz} \end{bmatrix} \tag{2-66}$$

with

$$\Omega = \begin{bmatrix} 0 & 1 & 0 \\ -1 & 0 & 0 \\ 0 & 0 & 0 \end{bmatrix}.$$

The entries of the symmetric matrix U_{rr} are given by

$$U_{xx}= \frac{ks+\mu-1}{d^3} - \frac{\mu}{r^3} + \dot{\theta}^2 + \frac{3(1-\mu-ks)(x+R\mu)^2}{d^5} + \frac{3\mu(x-R(1-\mu))^2}{r^5}, \qquad (2\text{-}67)$$

$$U_{yy}= \frac{ks+\mu-1}{d^3} - \frac{\mu}{r^3} + \dot{\theta}^2 + \frac{3(1-\mu-ks)y^2}{d^5} + \frac{3\mu y^2}{r^5}, \qquad (2\text{-}68)$$

$$U_{zz}= \frac{ks+\mu-1}{d^3} - \frac{\mu}{r^3} + \frac{3(1-\mu-ks)z^2}{d^5} + \frac{3\mu z^2}{r^5}, \qquad (2\text{-}69)$$

$$U_{xy}= \frac{3(1-\mu-ks)(x+R\mu)y}{d^5} + \frac{3\mu(x-R(1-\mu))y}{r^5}, \qquad (2\text{-}70)$$

$$U_{xz}= \frac{3(1-\mu-ks)(x+R\mu)z}{d^5} + \frac{3\mu(x-R(1-\mu))z}{r^5}, \qquad (2\text{-}71)$$

$$U_{yz}= \frac{3(1-\mu-ks)yz}{d^5} + \frac{3\mu yz}{r^5}. \qquad (2\text{-}72)$$

The matrix A(t) can then be evaluated along the reference trajectory

The vector differential equation (2-64) governing the state variations from the nominal path has a solution of the form

$$\tilde{x}(t) = \Phi(t,t_0)\,\tilde{x}(t_0) \tag{2-73}$$

where $\Phi(t,t_0)$ is the state transition matrix at time "t" relative to time "t_0." The matrix Φ, then, represents the sensitivities of the states at time "t" to small changes in the initial conditions. It is determined by numerically integrating the matrix differential equation

$$\frac{d}{dt}\Phi(t,t_0) = \dot{\Phi}(t,t_0) = A(t)\,\Phi(t,t_0), \tag{2-74}$$

with initial conditions $\Phi(t_0,t_0) = I$, the 6x6 identity matrix. Thus, the nonlinear equations of motion in (2-26) through (2-28) and the matrix equation (2-74) combine to result in 42 first-order differential equations that can be simultaneously integrated numerically to determine the state vector and its associated transition matrix at any instant of time. The reference trajectories that are of interest in this research are generated by a numerical integration method that uses a differential corrections process developed by Howell and Pernicka.[12,26-30] The orbits include solar radiation pressure forces as formulated by Bell[31] specifically for an orbit associated with the interior Lagrange point in the Sun-Earth system. The numerical integration routines used in this work are fourth- and fifth-order Runge-Kutta formulas available in the 386-Matlab software package.[32]

F. Bounded Orbits Near Libration Points

The computation of bounded periodic and quasi-periodic orbits in the vicinity of libration points has been of increasing interest during the past 100 years. The accomplishments of Poincaré (1854-1912) include a significant body of work on families of bounded periodic

orbits in the planar CR3BP, the planar ER3BP, and the three-dimensional ER3BP. During the time per od 1913 to 1939, Professor Elis Strömgren and others at the Copenhagen Observatory computed a family of bounded periodic orbits for μ=.50 near a collinear libration point in the planar CR3BP.[4] Other researchers have constructed two-dimensional and three-dimensional bounded periodic and quasi-periodic orbits near Lagrange points; some have investigated stable periodic orbits in the vicinity of the collinear libration points.[1,2,5-8,12-22,25-31]

This section first discusses the stability of the libration points in the CR3BP and then the ER3BP. The construction of bounded orbits near the collinear Lagrange points is then summarized. Finally, the specific reference trajectories used in the orbit determination error analysis and station-keeping studies in this work are introduced.

1. Stability of the Libration Points in the CR3BP

The accomplishments of those researchers who have constructed bounded orbits near collinear libration points are particularly significant because the collinear points are considered "unstable" points of equilibrium but with (only) one mode producing positive exponential growth. Bounded motion in their vicinity, therefore, is determined by deliberately not exciting the unstable mode. A second mode produces negative exponential orbital decay and is also deliberately not excited. In the CR3BP, the remaining four eigenvalues are purely imaginary. The existence of initial conditions that result in only trigonometric (sinusoidal) functions as solutions means that the collinear libration points, while unstable, possess *conditional* stability (with proper choice of initial conditions) in the linear sense.[9]

The instability of the collinear libration points can be demonstrated by looking at a specific example formulated in the CR3BP. Earlier in this chapter, the equations of motion in the ER3BP were linearized about a nominal path to give the first-order variational equation (2-64) that includes the Jacobian matrix A(t). The entries of the matrix A(t) are then defined in equations (2-65) through (2-72). These equations can be simplified by assuming the CR3BP is valid; hence, $\ddot{\theta} = 0$ and $R = \dot{\theta} = 1$. Also, if the stability of the collinear points is to be determined, the reference solution can now be the (stationary) libration point of interest in the CR3BP. Under the assumptions of the CR3BP and the libration point reference solution, the Jacobian matrix A(t) is constant and can be denoted as the constant matrix A; stability measures such as eigenvalue analysis can then be accomplished.

For this analysis, the vector $\tilde{x}$ represents relatively small variations from a particular libration point of interest (L_i). The linear variational equation consequently may be written as

$$\dot{\tilde{x}} = A\,\tilde{x} \tag{2-74}$$

where $\tilde{x} = [\alpha\ \beta\ \gamma\ \dot{\alpha}\ \dot{\beta}\ \dot{\gamma}]^T$, and A is the constant Jacobian matrix. In order to compute the constant matrix A, nondimensional collinear libration point coordinates $(x_{Li},0,0)$ for the CR3BP are substituted into the matrix A. (The matrix A(t) is given by equations (2-65) through (2-72), and, under the assumptions that the CR3BP is valid and the given libration point is the nominal solution, it reduces to the constant matrix A.) The matrix A will obviously be numerically different for each of the five libration points of interest.

The following three linear equations result:

$$\ddot{\alpha} = 2\,\dot{\beta} + (2B+1)\,\alpha \tag{2-75}$$

$$\ddot{\beta} = (2-B)\beta - 2\,\dot{\alpha} \tag{2-76}$$

$$\ddot{\gamma} = (-B)\gamma \tag{2-77}$$

where

$$B = \frac{1-\mu+ks}{[x_{L1}+\mu]^3} + \frac{\mu}{[x_{L1}+\mu-1]^3}, \tag{2-78}$$

and x_{L1} represents the nondimensional coordinate of the collinear libration point of interest. The variational equation for the out-of-plane component γ decouples from the in-plane equations and represents pure oscillatory motion. The equations in terms of α and β produce the characteristic equation

$$\lambda^4 + (2-B)\lambda^2 + (1+B-2B^2) = 0 \tag{2-79}$$

with roots that depend on the sign of $(2-B+2B^2)$. For the three collinear Lagrange points, the sign of this term is negative for all values of the mass ratio such that $0 \leq \mu \leq .5$. Consequently, the characteristic equation (2-79) has roots that include a purely imaginary pair and a real pair, opposite in sign. The solution of the linear variational equations (2-75), (2-76), and (2-77) for any of the collinear points then shows unbounded motion (exponential growth) in response to *arbitrary* initial conditions. The benefits of selecting

specific initial conditions to avoid exciting the unbounded exponential modes will be discussed later in this section. But first, a short paragraph discussing stability of the triangular Lagrange points in the CR3BP is included because the discoveries of natural satellites orbiting near triangular libration points has helped spur the current substantial interest in libration point spacecraft orbits.

The triangular libration points are marginally stable in the linear sense for a specific range of primary mass ratio in the CR3BP. Purely imaginary roots in two conjugate pairs are obtained for $\mu \leq .0385$, which is given here to four decimal places and is sometimes referred to as Routh's value.[4] The mass ratios (listed here to three decimal places), for example, in the three-body systems of the Earth-Moon ($\mu = 1.216 \times 10^{-6}$), Sun-Earth+Moon ($\mu = 3.022 \times 10^{-6}$) and Sun-Jupiter ($\mu = 9.485 \times 10^{-4}$) all satisfy the mass ratio requirement for marginal stability of the triangular points in the linearized model. Natural satellites, such as the Trojan asteroids or a moon of Saturn, occupy linearly stable orbits near triangular libration points in their respective systems.

2. Stability of the Libration Points in the ER3BP

Several researchers have analyzed the stability of the libration points in the elliptic problem, where both the mass ratio, μ, and the primary orbit eccentricity, e, influence stability.[4,9,33-35] The instability of the collinear libration points as determined in the circular problem for all the values of mass parameter persists for the elliptic problem; an analysis of the collinear points shows instability for any combination of the values of both μ and e.

The results of a linearized stability analysis regarding the effects of eccentricity and mass ratio on the linear stability of the triangular points have been published by Danby[34] and then later by Bennett[35]. Both Danby and Bennett have numerically generated graphic depictions of the linear stability region in the μ-e plane. For the

eccentricity in the Sun-Earth+Moon ER3BP, the value of μ which ensures linear stability is only slightly less than Routh's value (decreased by approximately one percent). An interesting aspect of the μ-e stability region is that a range of values of μ greater than Routh's value also defines a region of linear stability for a specific range of values of e less than .3143.

3. Construction of Bounded Collinear Libration Point Orbits

The initial goal in the process of generating bounded orbits near a collinear (unstable) libration point is to avoid exciting the unstable mode associated with the linearized motion. The meteoric dust particles that may be orbiting near Lagrange point L_2 in the Sun-Earth system could only linger near that point if they arrive with the "correct" initial position and velocity states relative to L_2. The "correct" initial conditions will only (primarily) excite the stable modes associated with the linearized motion and not (or minimally) excite the unstable mode. The degree to which the unstable mode is excited will determine the length of time that the dust particles linger near L_2. The general solution to the harmonic equation (2-77) is written

$$\gamma(t) = B_1 \cos(\nu t) + B_2 \sin(\nu t) \qquad (2\text{-}81)$$

where B_1 and B_2 are constants of integration, with values determined by initial conditions, and $\nu = (B)^{1/2}$. The coupled in-plane equations have eigenvalues of the form $i\lambda$, $-i\lambda$, η, $-\eta$ for $\lambda>0$ and $\eta>0$ where $i = (-1)^{1/2}$. They, therefore, yield solutions

$$\alpha(t) = A_1 e^{\eta t} + A_2 e^{-\eta t} + A_3 \cos(\lambda t) + A_4 \sin(\lambda t), \qquad (2\text{-}82)$$

$$\beta(t) = -C_1 A_1 e^{\eta t} + C_1 A_2 e^{-\eta t} + C_2 A_4 \cos(\lambda t) - C_2 A_3 \sin(\lambda t) \qquad (2\text{-}83)$$

where

$$C_1 = \frac{1}{2\eta}\ (1 + 2B - \eta^2),\ C_2 = \frac{1}{2\lambda}\ (1 + 2B + \lambda^2) \qquad (2\text{-}84)$$

and A_1, A_2, A_3, A_4 are constant coefficients, dependent on the given initial conditions. For bounded motion, the coefficient A_1 must be zero. For both periodic and quasi-periodic motion, A_2 must also be zero. These two restrictions eventually lead to two equations that the initial conditions must satisfy in order to produce a linear solution that is bounded. The initial conditions are denoted α_0, β_0, $\dot{\alpha}_0$, $\dot{\beta}_0$.

The constant coefficients (A_1,A_2,A_3,A_4) can then be treated as unknowns and expressed in terms of the initial conditions. Both A_1 and A_2 will be zero if[4]

$$A_1 = F_1\ \alpha_0 + F_2\ \beta_0 + F_3\ \dot{\alpha}_0 - .5\ \dot{\beta}_0 = 0 \qquad (2\text{-}85)$$

$$A_2 = F_1\ \alpha_0 - F_2\ \beta_0 - F_3\ \dot{\alpha}_0 - .5\ \dot{\beta}_0 = 0 \qquad (2\text{-}86)$$

where

$$F_1 = \frac{\lambda C_2}{2(\lambda C_2 - \eta C_1)}\ ;\ F_2 = \frac{-\lambda}{2(\eta C_2 + \lambda C_1)}\ ;\ \text{and}\ F_3 = .5\ C_2. \qquad (2\text{-}87)$$

When equations (2-85) and (2-86) are satisfied, the sinusoidal solutions to the linear equations (2-75), (2-76), and (2-77) can be

written in more compact form (using trigonometric identities) as

$$\alpha(t) = -A_x \cos(\lambda t + \phi), \tag{2-89}$$

$$\beta(t) = C_2 A_x \sin(\lambda t + \phi), \tag{2-90}$$

$$\gamma(t) = A_z \sin(\nu t + \psi), \tag{2-91}$$

$$A_x = (A_3^2 + A_4^2)^{1/2}, \tag{2-92}$$

$$A_z = (B_1^2 + B_2^2)^{1/2}, \tag{2-93}$$

$$\tan(\phi) = -(A_4 / A_3), \tag{2-94}$$

$$\tan(\psi) = (B_1 / B_2). \tag{2-95}$$

The linear solution can be very useful in developing a higher-order approximation to the actual nonlinear trajectory. The motion represented by the linearized solution as it appears above will be quasi-periodic since λ and ν are, in general, not equal. They are, however, of the same order of magnitude for the problem of interest. Periodic motion can be constructed by modifying equation (2-77) to force a solution with equal in-plane and out-of-plane frequencies:[17]

$$\ddot{\alpha} = 2\,\dot{\beta} + (2B+1)\,\alpha \tag{2-96}$$

$$\ddot{\beta} = (2-B)\beta - 2\,\dot{\alpha} \tag{2-97}$$

$$\ddot{\gamma} + \lambda^2\gamma = 0. \tag{2-98}$$

Equation (2-98) is derived by adding $(\lambda^2 - B)\gamma$ to the left-hand side of equation (2-77); the addition of this term is compensated for by using the higher-order terms in the analytic approximation. Specifically, periodic linear motion can be obtained if the in-plane (A_x) and out-of-plane (A_z) amplitudes of the motion are related in such a way that allows nonlinear contributions (higher-order terms in the analytic approximation) to the system to produce eigenfrequencies that are, in fact, equal.[17] The resulting linearized periodic equations would be of the form

$$\alpha(t) = -A_x \cos(\lambda t + \phi) \tag{2-99}$$

$$\beta(t) = C_2 A_x \sin(\lambda t + \phi) \tag{2-100}$$

$$\gamma(t) = A_z \sin(\lambda t + \psi). \tag{2-101}$$

The third-order analytic representation is used in this work to provide the initial model for the trajectories. The method of successive approximations, using the linearized solution as the first approximation to the nonlinear orbital path, and the method of dual time scales are used to derive the third-order result.[15,16,25] The method of successive approximations is used to generate an asymptotic series in an appropriately small parameter. (The square root of the eccentricity of the primary orbit, that is the orbit of the Earth-Moon

barycenter about the Sun, is the small parameter used here.) The method of dual time scales is used to convert the system of ordinary differential equations into a system of partial differential equations. In general, the method of multiple scales allows the various nonlinear resonance phenomena to be included in the approximate analytic solution and provides a method to remove secular terms. (Here, "secular" refers to terms that include the time variable and is derived from the French "siècle" meaning century.)

The analytic solution of Richardson and Cary[25] for the Sun-Earth+Moon ER3BP has been derived to fourth order, but the third-order approximation is found to be sufficient for this research.[12,26-30] A numerical integration algorithm, using a differential corrections procedure that is designed to adjust the first guess as obtained from the analytic approximation, can then be used to numerically generate the orbit of interest. A method developed by Howell and Pernicka[12,26-30] is used here to generate the orbital paths. Their method initially employs the approximate analytic solution to compute target points. A two-level (position matching then velocity matching), multi-step differential corrections algorithm is used to construct a numerically integrated, bounded trajectory that is continuous in position and velocity. A solar radiation pressure model developed by Bell[31] is also incorporated in the numerical integration procedure.

The method of Howell and Pernicka, including solar radiation pressure, uses an initial analytic guess that represents a halo orbit or, alternatively, a considerably smaller Lissajous path. The higher-order terms tend to slightly alter the first-order periodic or quasi-periodic path. Consequently, the initial target path for a halo orbit will generally not be precisely periodic. The two-level, multi-step differential corrections procedure then adjusts the initial analytic target orbit and, therefore, will compute a halo-type orbit that is nearly (but not exactly) periodic.

4. The Reference Paths Generated for This Work

An original goal of this research was to compare orbit determination error analysis results and station-keeping costs for Lissajous and halo orbits. Precisely periodic halo orbits exist in the CR3BP. They also exist in the ER3BP, but, in the ER3BP, they are multiple revolution trajectories with periods much longer than those of interest here. Nearly periodic orbits are more practical in the ER3BP and are much more likely to be used in mission planning; therefore, the goal here should be slightly modified to be the comparison of Lissajous and "halo-type" orbits. The general shapes of the three-dimensional halo-type and Lissajous orbits can be seen by plotting three orthographic views of each orbit, using the tabular data from the numerical integration routine. Figure 2-4 depicts three orthographic views of point plots for the Lissajous orbit used in this research. Figure 2-5 contains three orthographic views (on a slightly different scale) of the considerably larger halo-type orbit to be used later in this work. (Note that, in general, the amplitude ratio for Lissajous trajectories is arbitrary. In halo orbits, however, constraining the amplitude ratio results in equalized frequencies for in-plane and out-of-plane motion.) The orbits are depicted in the rotating reference frame centered at L_1.

Both orbits are clearly not periodic; a Lissajous orbit is often called a quasi-periodic path, and these two orbits could clearly be termed quasi-periodic or Lissajous paths. The major difference between the orbits is the larger size of the halo-type orbit; however, other differences are also present. The maximum x and y excursions of the halo-type orbit are approximately four times as large as those of the Lissajous path. Furthermore, the direction of motion (clockwise versus counterclockwise), as viewed in the y-z orthographic depiction, is different for the two orbits used here. The direction of motion on the halo-type orbit is counterclockwise in the y-z depiction; the direction of motion is clockwise in the y-z depiction for the Lissajous path. (Both orbits include clockwise motion in the x-y depiction.)

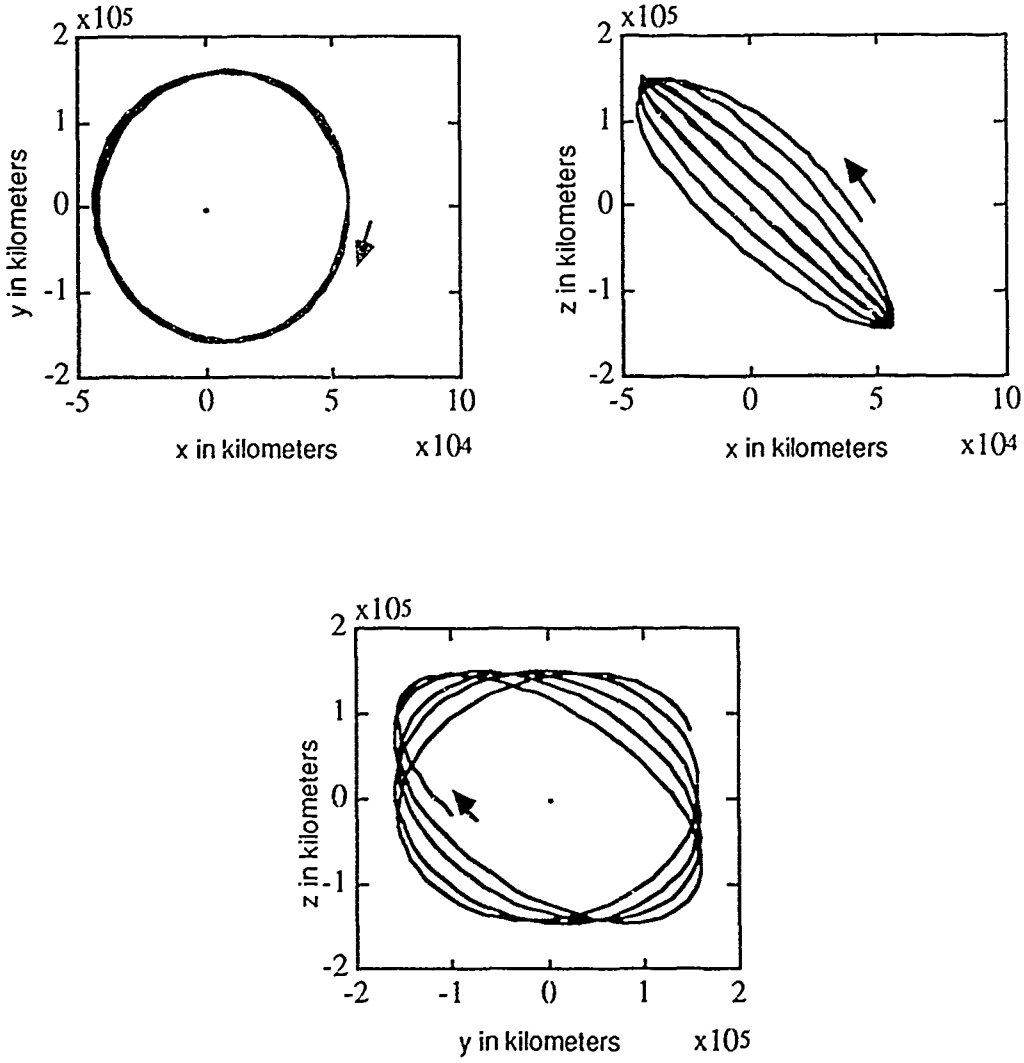

Indicates the direction of motion.

Indicates the location of the libration point.

Figure 2-4. Three Orthographic Views of a Lissajous Orbit.

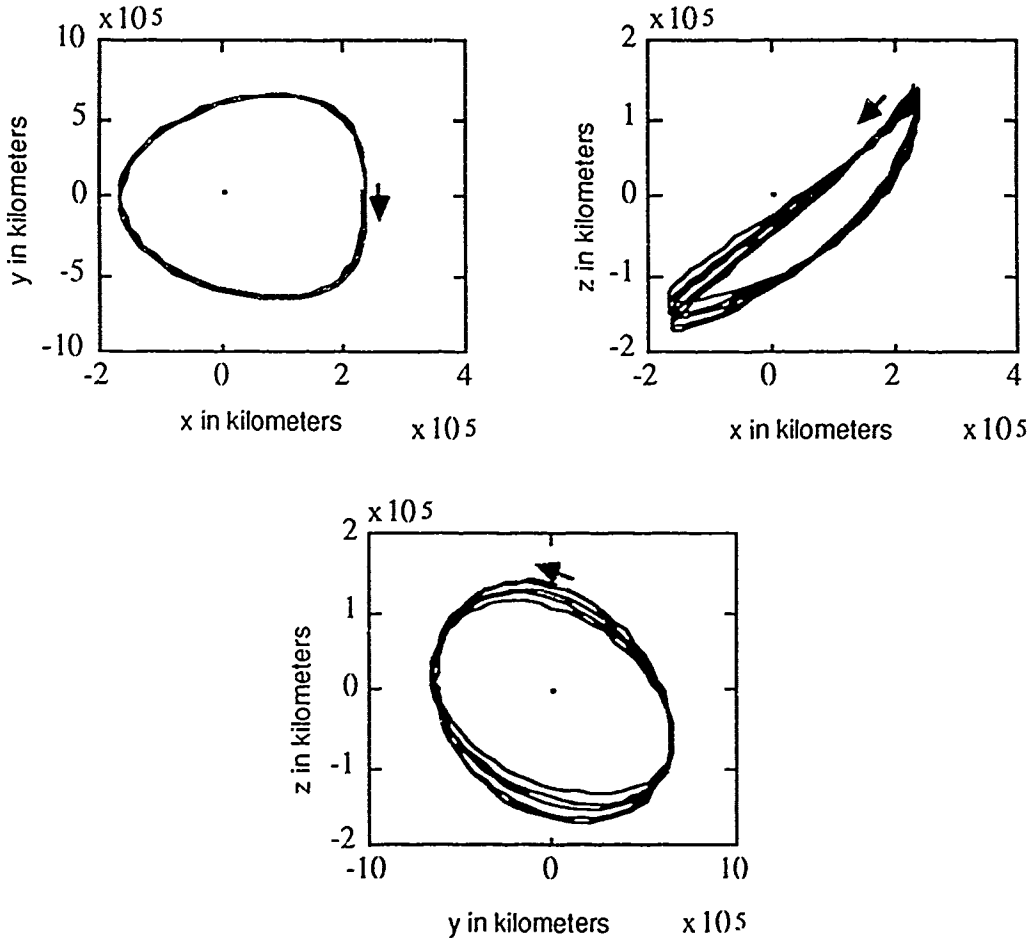

indicates direction of motion.

. indicates the libration point location.

Figure 2-5. Three Orthographic Views of a Halo-Type Orbit.

The two orbits can also be differentiated in terms of the direction of the maximum z excursion in the x-z depiction. If the maximum z excursion is in the positive z direction, the orbit can be termed a member of a "northern family" of orbits. When the maximum z excursion of the orbit is in the negative z direction, the orbit is termed a member of a "southern family" of orbits. In the x-z orthographic depiction, the smaller (Lissajous) path can be seen to be a member of a northern family of orbits, while the halo-type orbit is a member of a southern family of orbits.

The differences in the paths, outlined in the preceeding paragraphs, are the consequences of the initial conditions selected for the numerical integration of the trajectory. The initial conditions used for computation of the orbit near libration point L_1 determine the related characteristics of direction of motion in the y-z plane and the family of orbits (northern or southern) to which it belongs.

CONCLUSION

The restricted three-body problem is an important and interesting area of research. The Sun-Earth+Moon ER3BP, in particular is currently an area of vital research attention. The addition of solar radiation pressure in the Sun-Earth+Moon ER3BP alters the locations and the conditions for linear stability of the Lagrange points. Including these solar effects improves the accuracy of the dynamic model, but there are also additional, related benefits. Simulations used to calculate expected tracking errors and the cost of maintaining the spacecraft near the unstable orbits can now also include uncertainty in this solar radiation pressure force. The addition of this real uncertainty will, in turn, improve the accuracy of further studies conducted in relation to future spacecraft missions.

LIST OF REFERENCES

1. G.H. Darwin, "Periodic Orbits," *Acta Mathematica*, Volume 21, 1899, pages 99-242.

2. G.H. Darwin, "Periodic Orbits," *Scientific Papers*, Volume 4, Cambridge University Press, Cambridge, Massachusetts, 1911.

3. R.H. Battin, *An Introduction to the Mathematics and Methods of Astrodynamics*, AIAA Education Series, New York, 1987.

4. A.E. Roy, *Orbital Motion*, Second Edition, Adam Hilger Ltd, Bristol, England, 1982.

5. H.C. Plummer, "On Oscillating Satellites-1," *Monthly Notices of the Royal Astronomical Society*, Volume 63, Number 8, 1903, pages 436-443.

6. H.C. Plummer, *An Introductory Treatise on Dynamical Astronomy*, Cambridge Press, London, 1918.

7. F.R. Moulton, *An Introduction to Celestial Mechanics*, Second Revised Edition, The Macmillan Company, New York, 1914.

8. F.R. Moulton, "Periodic Orbits," Carnegie Institute of Washington Publications, Number 161, 1920.

9. V. Szebehely, *Theory of Orbits: The Restricted Problem of Three Bodies*, Academic Press, New York, 1967.

10. "A Weather Eye on the Sun," *The Economist*, December 8, 1990, pages 95,96.

11. G. Parks, S. Shawhan, M. Calabrese, J. Alexander, "Global Geospace Science Program," *Journal of the British Interplanetary Society*, Volume 41, 1988, pages 81-93.

12. H.J. Pernicka, "The Numerical Determination of Nominal Libration Point Trajectories and Development of a Station-Keeping Strategy," PhD Dissertation, School of Aeronautics and Astronautics, Purdue University, West Lafayette, Indiana, May 1990.

13. R.W. Farquhar, "The Control and Use of Libration-Point Satellites," Ph.D. Dissertation, Department of Aeronautics and Astronautics, Stanford University, Stanford, California, July 1968.

14. R.W. Farquhar, "A Halo-Orbit Lunar Station," *Astronautics and Aeronautics*, June 1972, pages 59-63.

15. R.W. Farguhar and A.A. Kamel, "Quasi-Periodic Orbits About the Translunar Libration Point," *Celestial Mechanics*, Volume 7, 1973, pages 458- 473.

16. D.L. Richardson, "Analytic Construction of Periodic Orbits About the Collinear Points," *Celestial Mechanics*, Volume 22, 1980, pages 241-253.

17. D.L. Richardson, "Halo Orbit Formulation for the ISEE-3 Mission," *Journal of Guidance and Control*, Volume 3, Number 6, November-December 1980, pages 543-548.

18. C.G. Zagouras and P.G. Kazantzis, "Three Dimensional Periodic Oscillations Generating from Plane Periodic Ones Around the Collinear Lagrangian Points," *Astrophysics and Space Science*, Volume 61, Number 2, April 1979.

19. J.V. Breakwell and J.V. Brown, "The 'Halo' Family of 3-Dimensional Periodic Orbits in the Earth-Moon Restricted Three-Body Problem," *Celestial Mechanics*, Volume 20, 1979, pages 389-404.

20. K.C. Howell, "Three Dimensional, Periodic Halo Orbits in the Restricted Three-Body Problem," Ph.D. Dissertation, Department of Aeronautics and Astronautics, Stanford University, Stanford, California, March 1983.

21. K.C. Howell and J.V. Breakwell, "Almost Rectilinear Halo Orbits," *Celestial Mechanics*, Volume 32, 1984, pages 29-52.

22. K.C. Howell, "Three Dimensional, Periodic, 'Halo' Orbits," *Celestial Mechanics*, Volume 32, 1984, pages 53-71.

23. J.R. Wertz, Editor, *Spacecraft Attitude Determination and Control*, D. Reidel Publishing Co, Boston, 1978.

24. S. Wolf, *Guide to Electronic Measurements and Laboratory Practice*, Prentice Hall, Englewood Cliffs, New Jersey, 1973.

25. D.L. Richardson and N.D. Cary, "A Uniformly Valid Solution for Motion About the Interior Libration Point of the Perturbed Elliptic-Restricted Problem," AAS/AIAA Astrodynamics Specialists Conference, Nassau, Bahamas, July 28-29, 1975, AAS Paper 75-021.

26. H.J. Pernicka, "The Numerical Determination of Lissajous Orbits in the Circular Restricted Three-Body Problem," M.S. Thesis, School of Aeronautics and Astronautics, Purdue University, West Lafayette, Indiana, December 1986.

27. K.C. Howell and H.J. Pernicka, "Numerical Determination of Lissajous Trajectories in the Restricted Three-Body Problem," *Celestial Mechanics*, Volume 41, 1988, pages 107-124.

28. K.C. Howell, Principal Investigator, "Trajectory Design for Libration Point Trajectories and for Double Lunar Swingby Trajectories," Final Report Prepared for Computer Sciences Corporation, December 1987.

29. K.C. Howell, Principal Investigator, "Design of Libration Point Trajectories and Consecutive Lunar Encounter Trajectories," Final Report Prepared for Computer Sciences Corporation, September 1988.

30. H.J. Pernicka, "The Numerical Determination of Libration Point Trajectories, Including Development of Station-Keeping Strategies," Proposal for Dissertation, School of Aeronautics and Astronautics, Purdue University, West Lafayette, Indiana, December 1988.

31. J.L. Bell, Private Communication, School of Aeronautics and Astronautics, Purdue University, West Lafayette, Indiana, August, 1990.

32. The MathWorks, *386-Matlab*, 21 Eliot Street, South Natick, Ma, 1989.

33. E.A. Grebenikov, "On the Stability of the Lagrangian Triangle Solutions of the Restricted Elliptic Three-Body Problem," *Soviet Astronomy*, Volume 8, Number 3, November-December 1964, pages 567-578.

34. J.M.A. Danby, "Stability of the Triangular Points in Elliptic Restricted Problem of Three Bodies," *The Astronomical Journal*, Volume 69, Number 2, March 1964, pages 165-172.

35. A. Bennett, "Characteristic Exponents of the Five Equilibrium Solutions in the Elliptically Restricted Problem," *Icarus*, Volume 4, 1965, pages 177-190.